Sedimentary Geology 333 (2016) 32–49

Contents lists available at ScienceDirect

Sedimentary Geology

journal homepage: www.elsevier.com/locate/sedgeo

# Oroclinal bending of the Juan Fernández Ridge suggested by geohistory analysis of the Bahía Inglesa Formation, north-central Chile

Jacobus P. Le Roux [a,b,*], Luciano Achurra [c], Álvaro Henríquez [d], Catalina Carreño [e], Huber Rivera [a], Mario E. Suárez [f], Scott E. Ishman [g], Nicholas D. Pyenson [h,i], Carolina S. Gutstein [h,i,j]

[a] Departamento de Geología, Facultad de Ciencias Físicas y Matemáticas Universidad de Chile, Plaza Ercilla 803, Santiago, Chile
[b] Andean Geothermal Centre of Excellence, Plaza Ercilla 803, Santiago, Chile
[c] Arcadis Consultores, Santiago, Chile
[d] SQM, S.A., Calama, Chile
[e] Codelco, Calama, Chile
[f] Laboratorio de Ontogenia y Filogenia, Facultad de Ciencias, Universidad de Chile, Santiago, Chile
[g] Department of Geology, Southern Illinois University, Carbondale, IL, USA
[h] Department of Paleobiology, National Museum of Natural History, Smithsonian Institution, PO Box 37012, Washington, DC 20013, USA
[i] Department of Mineral Sciences, National Museum of Natural History, Smithsonian Institution, PO Box 37012, Washington, DC 20013, USA
[j] Comisión de Patrimonio Natural, Consejo de Monumentos Nacionales, Av. Vicuña Mackenna 84, Providencia, Santiago, Chile

ARTICLE INFO

*Article history:*
Received 11 September 2015
Received in revised form 1 December 2015
Accepted 9 December 2015
Available online 17 December 2015

Editor: Dr. B. Jones

*Keywords:*
Rocky shoreline deposits
Tsunami deposits
Juan Fernández Ridge
Copiapó Ridge
Copiapó ignimbrite
*Bulimina marginata*

ABSTRACT

The stratigraphy of the Bahía Inglesa Formation in the Caldera Basin west of Copiapó, (north-central Chile) is revised, based on hitherto unpublished stratigraphic sections and $^{87}Sr/^{86}Sr$ dating. The depositional environment varied from a rocky shoreline to the upper continental slope, with sea-level oscillations and tectonic movements causing numerous local unconformities as well as lateral and vertical facies changes. Geohistory and sedimentological analyses show that the area was close to the concurrent sea level at about 15.3 Ma, but at the same time being elevated about 100 m above the present sea level. Although the basin then subsided at least 350 m until around 6 Ma, marine deposition was only recorded after 10.4 Ma. This suggests that the sea level initially dropped faster than the rate of subsidence so that subaerial erosion occurred. The period of subaerial exposure before 10.4 Ma can be attributed to the presence of a NE-trending branch of the Juan Fernández Ridge below the continental crust at this time, whereas the ensuing subsidence was due to subduction erosion and crustal accommodation in its wake as it migrated south along the South American coastline. The subsequent uplift of at least 250 m can be explained by an acceleration in plate expansion and isostatic rebound of the continental crust after being partially submerged in the upper mantle. The uplift–subsidence–uplift pattern mirrors those recorded around the Nazca Ridge in Peru, as well as in similar basins to the south of Caldera. However, a higher southward migration rate of the Juan Fernández Ridge against the edge of the South American Plate and less intense uplift–subsidence–uplift cycles are recorded in the latter basins. This can possibly be attributed to oroclinal bending of the ridge due to friction with the overlying continental plate, which diminished the angle of incidence and the intensity of the stress field, but increased the migration velocity of the ridge relative to the coastline.



## 1. Introduction

A prominent feature of the Pacific coastline of South America between 2° and 47°S is the presence of Neogene sedimentary basins with similar structural and sedimentological characteristics (Fig. 1). In Chile, during the last few decades, many of these basins have been studied intensively (e.g. Marquardt, 1999; Hartley et al., 2001; Godoy et al., 2003; Gómez, 2003; Le Roux et al., 2004, 2005a,b, 2006, 2008; Marquardt et al., 2004; Suárez et al., 2004, 2006; Walsh and Suárez, 2005, 2006; Encinas, 2006; Walsh and Martill, 2006; Finger et al., 2007; Sallaberry et al., 2007; Encinas et al., 2008, 2010; Gutiérrez, 2011; Carreño, 2012; Gutiérrez et al., 2013; Pyenson et al., 2014). In spite of this effort, however, many uncertainties still remain with regard to their ages, depositional environments, and inter-basinal correlations (e.g. Finger et al., 2013; Le Roux et al., 2013, 2014; Encinas et al., 2014; Spiske et al., 2014; Le Roux, 2015). Here, we present an interpretation of the stratigraphy, age, depositional environment, and tectonic setting of the Bahía Inglesa Formation in the Caldera Basin west of Copiapó, based on as yet unpublished stratigraphic sections measured throughout the basin (Le Roux, unpublished work, Achurra, 2004; Henríquez, 2006; Carreño, 2012).

* Corresponding author at: Departamento de Geología, Universidad de Chile, Plaza Ercilla 803, Santiago, Chile.
*E-mail address:* jroux@cec.uchile.cl (J.P. Le Roux).

http://dx.doi.org/10.1016/j.sedgeo.2015.12.003
0037-0738/

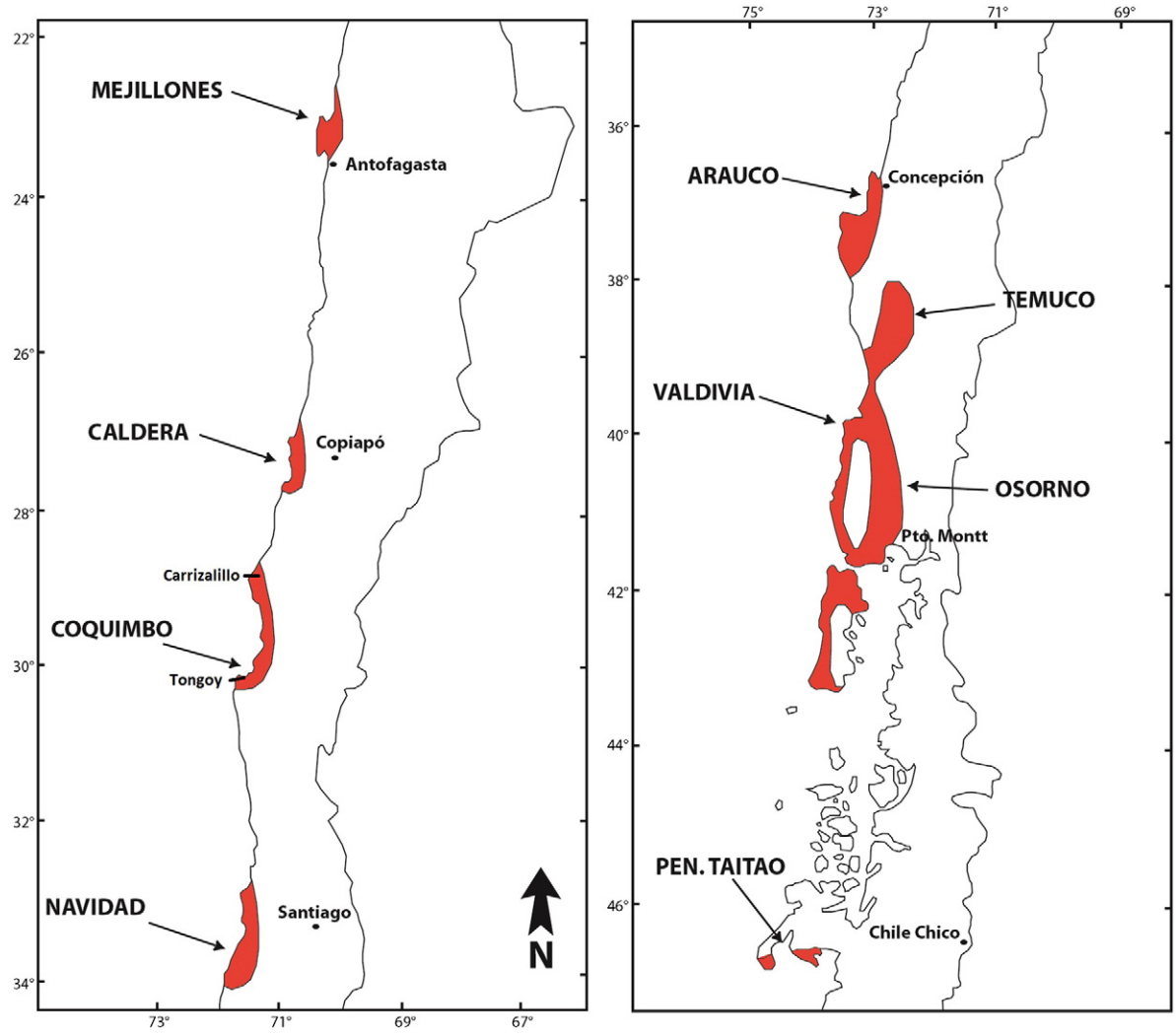


**Fig. 1.** Neogene sedimentary basins along the Chilean coastline.

## 2. Geological background and previous work

The Caldera Basin is located at the northern margin of the so-called flat slab region, which is characterized by low-angle subduction probably related to the presence of multiple ocean ridges (Pardo et al., 2002; Le Roux et al., 2005a). The basin developed over a distance of 43 km on the coastal plain between Caldera and the mouth of the Copiapó River, with a maximum width of about 20 km from the coastline to the Coastal Range (Fig. 2). It is filled by a Neogene marine succession directly overlying Paleozoic metamorphic rocks and Mesozoic granitoids (Marquardt, 1999; Godoy et al., 2003).

Three Neogene units have been identified within this basin (Rojo, 1985; Marquardt, 1999; Godoy et al., 2003; Marquardt et al., 2004), namely, the Angostura Formation, the Bahía Inglesa Formation, and the Caldera Beds. The Bahía Inglesa Formation, cropping out between the Copiapó and Caldera Bays (Fig. 2), is a semi-consolidated succession of (bio)clastic and phosphatic rocks characterized by numerous lateral and vertical facies changes. Near Puerto Viejo (Fig. 3), it unconformably overlies the Angostura Formation of early to middle Miocene age (Marquardt et al., 2000). Further north, at Playa Chorrillos (section 17 in Fig. 3), it has a non-conformable contact with the Jurassic Morro Copiapó Granodiorite (Fig. 2). It is overlain, in turn, by the Pleistocene Caldera Beds (Gutstein et al., 2009; Valenzuela-Toro et al., 2013).

Different authors have dated the Bahía Inglesa Formation on the basis of shark teeth (Rojo, 1985; Suárez et al., 2004; Suárez, 2015), paleomalacology (Herm, 1969; Mortimer, 1969; Guzmán et al., 2000), micropaleontology (Herm, 1969; Marchant et al., 2000; Achurra, 2004; Henríquez, 2006), morphostratigraphic relationships (Marquardt, 1999; Marquardt et al., 2000), K-Ar dating (Marquardt, 1999), and Sr isotopes (Achurra, 2004; Henríquez, 2006) as middle Miocene to Pliocene. Recently, a rich fossil mammal site (Cerro Ballena, section 32 in Fig. 3) was age-bracketed by Pyenson et al. (2014) on the basis of co-existing shark and aquatic sloth species as late Tortonian to early Messinian. The Caldera Beds at the same location have yielded macrofossils of Pleistocene age (Long, 1993; Suárez et al., 2010; Valenzuela-Toro et al., 2013).

The depositional environment has been interpreted as ranging from the littoral zone to the upper continental slope (about 800 m depth) based on benthic foraminifers (Achurra, 2004; Henríquez, 2006) and sedimentary facies (Marquardt, 1999; Walsh and Hume, 2001; Godoy et al., 2003; Achurra, 2004; Henríquez, 2006; Walsh and Suárez, 2006; Achurra et al., 2009).

More than 60 species of vertebrates have been recorded from the phosphatic bonebeds south ofCaldera (Suárez et al., 2002, 2004; Suárez, 2015; Bianucci et al., 2006; Gutstein et al., 2007, 2008, 2015; Rubilar-Rogers et al., 2009; Valenzuela-Toro and Gutstein, 2015), including chondrichtyan fishes (sharks, rays, and chimeroids), reptiles (crocodiles), sea birds (penguins, albatrosses, boobies, cormorants, and petrels), marine mammals (whales, dolphins, seals, dugongs, and marine sloths) and continental mammals (capybaras). These

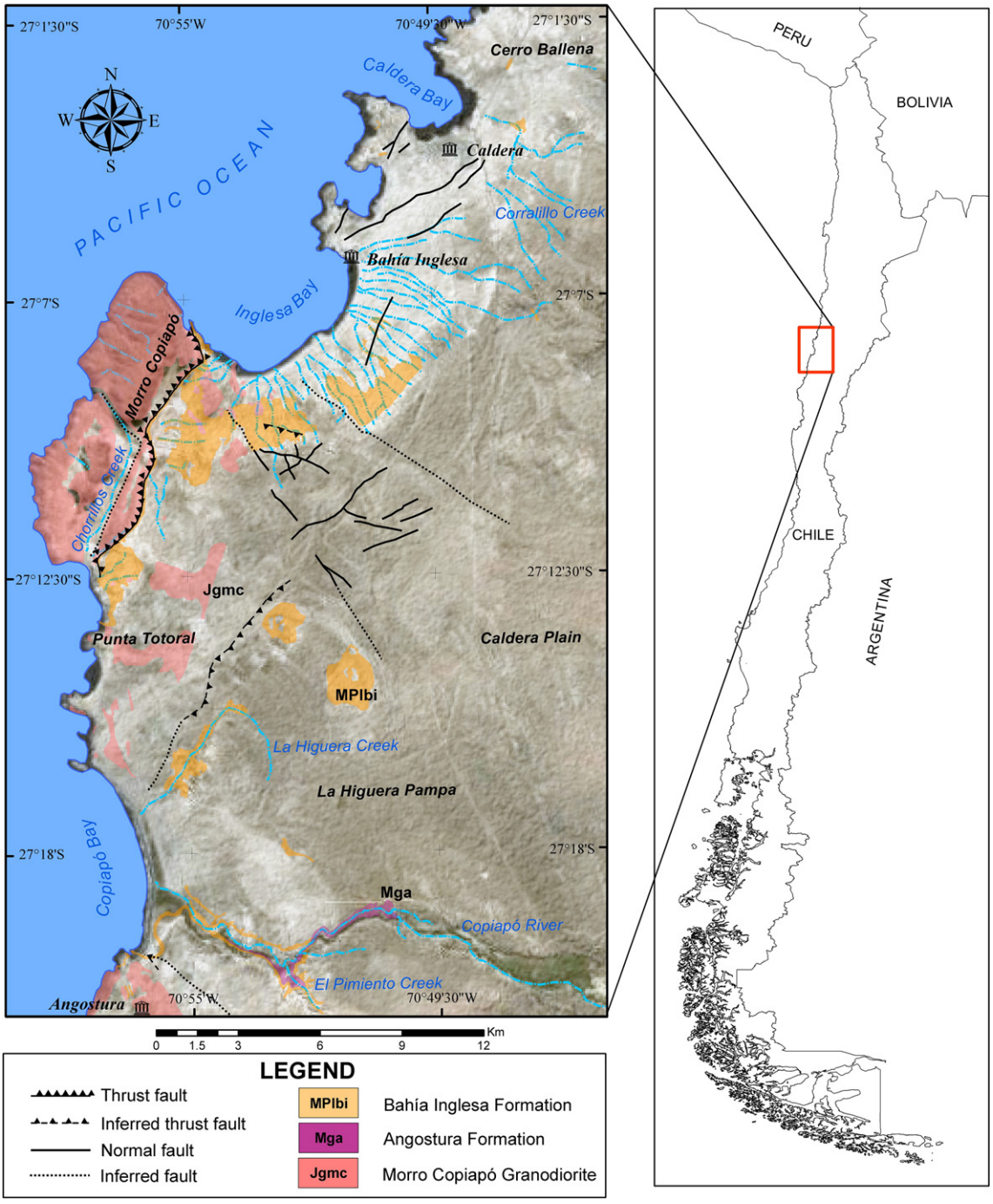


**Fig. 2.** Simplified geological map of the Caldera Basin (after Godoy et al., 2003), showing localities mentioned in text.

phosphatic bonebeds and the recent fossil whale discovery at Cerro Ballena represent some of the best preserved fossil sites in the world (Pyenson et al., 2014).

## 3. Stratigraphy

A total of 32 stratigraphic sections were measured in the Bahía Inglesa Formation since 2003 (Fig. 3; Appendix), but the majority of these profiles have only been recorded in unpublished graduate and masters theses (Achurra, 2004; Henríquez, 2006; Carreño, 2012). Of these, section 18 (Le Roux, unpublished work) lies within a submarine canyon cutting through older strata of the Bahía Inglesa Formation, so that the canyon-fill deposits cannot be correlated directly with the rest of the Bahía Formation profiles, even though they are considered to belong to the same succession.

Henríquez (2006) studied the area from just south of Puerto Viejo to Punta Totoral, whereas Le Roux (unpublished work), Achurra (2004), and Carreño (2012) examined the northern sector between Punta Totoral and Quebrada Blanca (sections 13 and 31). Fig. 3 shows the locations of the measured sections, numbered as 1–32 from south to north, whereas Table 1 compares these numbers with the original profile designations. The correlation of selected measured profiles across different parts of the basin is shown in the Appendix, in order to demonstrate the stratigraphic control used as a basis for the stratigraphic subdivision and geohistory analysis.

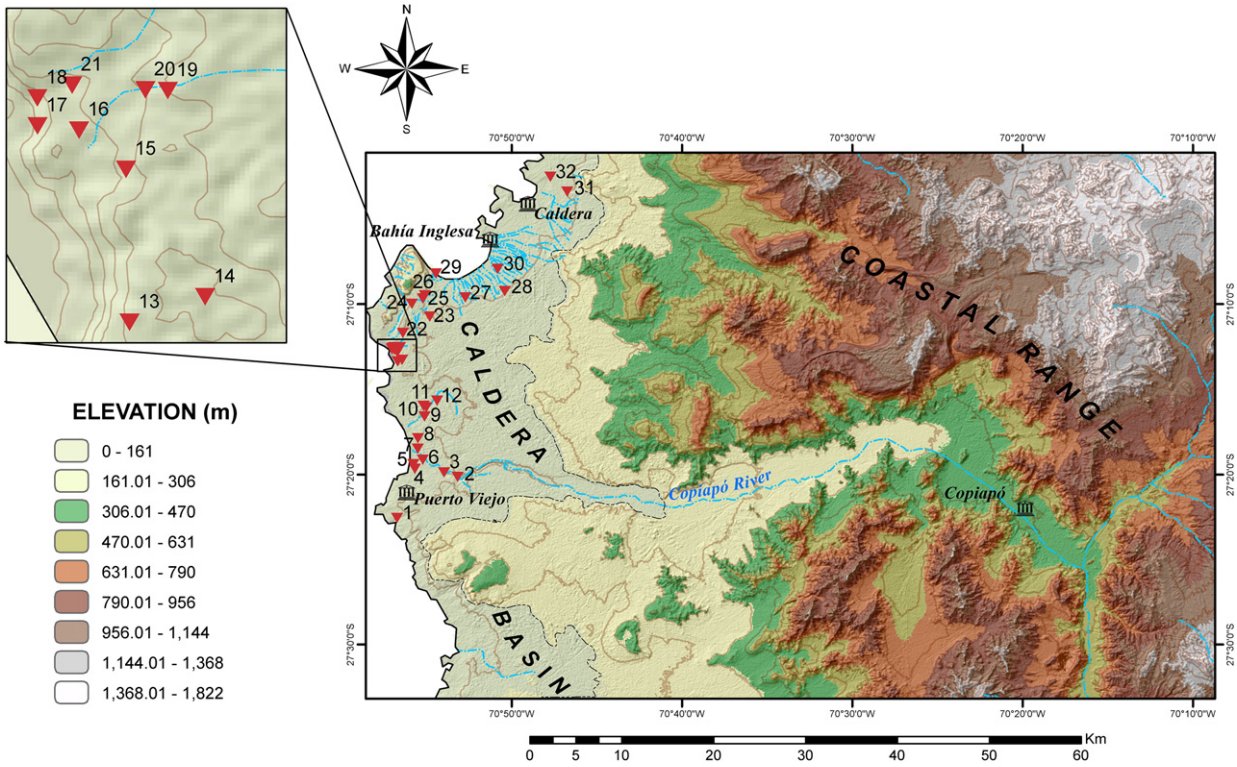


**Fig. 3.** Localities of measured stratigraphic sections between Puerto Viejo and Caldera: see Table 1 for original designations by Achurra (2004), Henríquez (2006), and Carreño (2012).

While Henríquez (2006) identified 13 units in his study area, Achurra (2004) and Carreño (2012) identified 8 and 9 units, respectively. These are here reinterpreted and subdivided into formal members with geographical names, according to the rules of the International Subcommission on Stratigraphic Classification of the IUGS Commission of Stratigraphy (Hedberg, 1976). Fig. 4 shows a composite stratigraphic succession of the Bahía Inglesa Formation based on selected, measured type sections of the different members.

**Table 1**
List of original measured sections and present designations numbered from 1 to 32. Locations are shown in Fig. 2. Letters in brackets indicate original author (H = Henríquez; A = Achurra; C = Carreño; L = Le Roux).

1. Quebrada Añañucal (H)
2. Desembocadura El Pimiento (H)
3. Quebrada Río Copiapó (H)
4. Quebrada Puerto Viejo (H)
5. Playa Norte Puerto Viejo (H)
6. Desembocadura Sur, Quebrada Copiapó (H)
7. Desembocadura Norte, Quebrada Copiapó (H)
8. Las Salinas (H)
9. Quebrada La Higuera (H)
10. Cerro Testigo, Quebrada la Higuera (H)
11. Cerro Extremo Norte, Quebrada La Higuera (H)
12. Corte Camino, Quebrada La Higuera (H)
13. Punta Totoral (H)
14. AL-1 (A)
15. Chorillos 4, CHO-4 (A)
16. Chorillos 3, CHO-3 (A)
17. Playa Chorillos Sur, PCS (L)
18. Playa Chorillos Norte, PCN (L)
19. LT-2 (A)
20. LT-1 (A)
21. Chorillos 1, CHO-1 (A)
22. Chorillos 8, CHO-8 (A)
23. Los Amarillos, LA (C)
24. El Morro 1, EM-1 (A)
25. El Morro, EM (C)
26. Quebrada El Morro, QEM-1 (A)
27. Mina Fosforita, MF (C)
28. Los Negros, LN (C)
29. Quebrada El Morro 3, QEM-3 (A)
30. Rocas Negras, RN-1 (A)
31. Quebrada Blanca, QBL-1 (A)
32. Cerro Ballena, CB (C, L)

### 3.1. Angostura Formation (units 1 and 2 of Henríquez, 2006)

The Angostura Formation is present along the lower reaches of the Copiapó River and possibly in an isolated outcrop in Quebrada La Higuera (Fig. 2; localities 2, 3, and 9 in Fig. 3). It is composed of two conglomerate units separated by an erosional contact.

The basal conglomerate (unit 1 of Henríquez, 2006) has an average thickness of 2.5 m, overlying the Jurassic basement gabbros with a non-conformable contact, and consists of fine, matrix-supported, horizontally stratified conglomerate with reddish, poorly sorted, angular granitoid clasts. The matrix is medium-grained sandstone that generally fines upward. Some bioclasts, mostly broken *Balanus* shells filling shallow channels, are present. Henríquez (2006) correlated only this part of the Angostura Formation (as defined here) with the Angostura Gravels, whereas Godoy and Lara (1998) noted an erosional contact between the latter and the overlying Bahía Inglesa Formation. It is not clear whether the latter authors considered the second conglomerate mentioned above to be part of the Bahía Inglesa Formation, or whether they referred to another conglomerate at the base of the El Pimiento Member. Whatever the case may be, the lower conglomerate unit has a middle Miocene age (Godoy et al., 2003), whereas the second conglomerate was dated by $^{87}Sr/^{86}Sr$ on a *Chlamys* specimen at 15.3 ± 0.6 Ma (Henríquez, 2006). Although erosional contacts are common among the different units of the Bahía Inglesa Formation, the 5-million-year age difference between the Angostura Formation and the El Pimiento Member (of which the basal part was dated at 10.4 ± 0.9 Ma by Henríquez, 2006), indicates a major unconformity, so that the upper conglomerate cannot be included as a member of the Bahía Inglesa Formation (Henríquez, 2006).

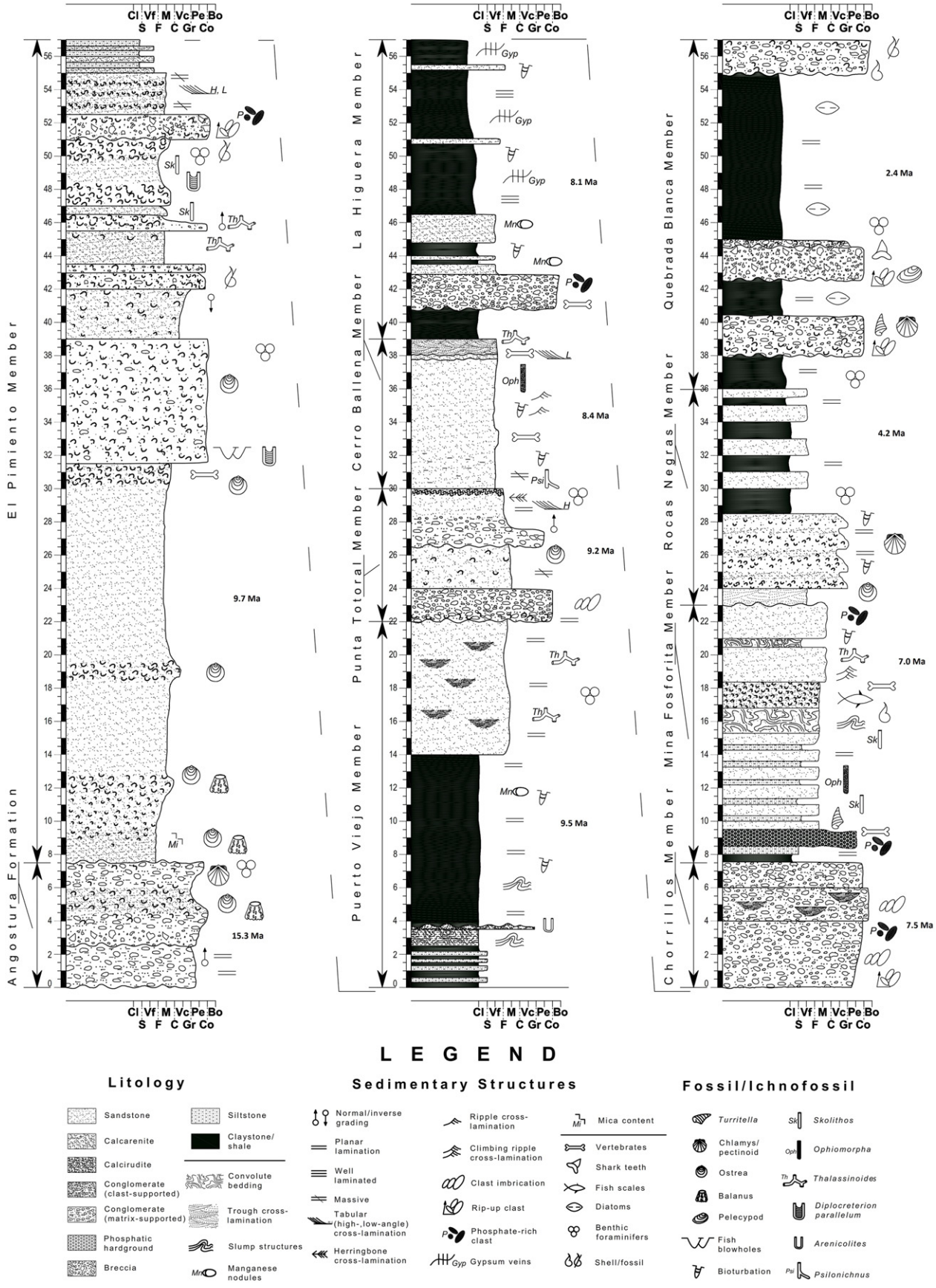


**Fig. 4.** Type sections of the different members of the Bahía Inglesa Formation. For location, see Fig. 3.

The upper part of the Angostura Member (unit 2 of Henríquez, 2006), reaches a thickness of about 5 m and has a polymictic, clast-supported conglomerate at the base, showing angular pebbles and cobbles in a medium-grained sandstone to gravelly matrix. It grades upward into very coarse, poorly sorted, matrix-supported conglomerate with subrounded boulders up to 1 m in diameter. The percentage of bioclasts (*Balanus*, *Ostrea*) gradually increases upward so that the rock grades into a biocalcirudite, before reverting again to a matrix-supported, polymictic conglomerate with bioclast fragments.

Benthonic foraminifer species recorded in the Angostura Formation include *Bolivina bicostata* Cushman 1937, *Bolivina pseudospissa*, *Buliminella elegantissima* d´Orbigny 1839, *Buliminella peruviana* Cushman and Stone 1947, and unidentified species of *Hoeglundia* and *Pseudononion*.

The presence of *Balanus*, *Ostrea*, and *Chlamys* shell fragments suggests marine interaction along the lower reaches of the paleo-Copiapó River, along which the Angostura gravels were transported from the continental hinterland. In the Central Valley of the Atacama Region of north-central Chile, the Angostura Gravel Formation (Mortimer, 1973) reaches a maximum thickness of about 500–600 m (Gabalda et al., 2005), where it was deposited in large alluvial fans. In the coastal sector, however, it has a very limited thickness (7.5 m), but it is still possible to show its distribution on a 1:50,000 map due to its horizontal disposition. Therefore, there is no need for a change in rank to that of a member, and in any case it does not form part of any formal formation at this locality.

### 3.2. Bahía Inglesa Formation

#### 3.2.1. El Pimiento Member (unit 1 and basal part of unit 2 of Achurra, 2004; units 3 and 5, basal part of unit 6 of Henríquez, 2006)

Henríquez (2006) identified three units (3–5) overlying his unit 2 (here included within the Angostura Member), but the contact between his units 4 and 5 were never directly observed in the field. Furthermore, the latter unit generally overlies the Jurassic basement directly (sections 4, 5, 6, 8, and 13), is lithologically similar to unit 3 (mainly biocalcarenites, biocalcirudites and sandstones), and was dated (according to stratigraphic position) at 10.3 ± 0.9 Ma (Table 3.3; Henríquez, 2006), which coincides with the $^{87}Sr/^{86}S$ age of 10.4 ± 0.9 Ma for his unit 3. Therefore, in the absence of evidence to the contrary, units 3 and 5 of Henriquez (*op cit.*) are here considered to be stratigraphically equivalent and to form part of the El Pimiento Member.

In sections 2 and 3, the El Pimiento Member (unit 3 of Henríquez, 2006) overlies the Angostura Member with a sharp to erosional contact. This up to 24-m-thick succession consists of grey, quartz-rich, medium-grained biocalcarenites and fine to medium, micaceous quartzarenites containing up to 15% *Ostrea*, *Balanus*, *Chlamys* and unidentified gastropod fragments. The contacts between these lithologies are gradual and the percentage of bioclasts decreases up the profile.

In section 4, the lower part of unit 6 of Henríquez (2006) is considered to belong to the upper part of the El Pimiento Member, which here consists of an up to 2-m-thick, well-imbricated conglomerate containing fine-grained sandstone, phosphate, and granitoid clasts with scarce shell fragments. This is followed by 2.5 m of grey, medium-grained sandstones with thin calcirudite intercalations showing low- and high-angle planar cross-lamination. The underlying unit 5 of Henríquez (2006) at this locality is also considered to be part of the El Pimiento Member, being composed of medium- to coarse-grained biocalcarenites and sandstones.

In the nearby section 5, unit 5 of Henríquez (2006) is up to 11 m thick, consisting mainly of medium- to coarse-grained, massive calcarenites with scarce bioclasts, as well as biocalcarenites and minor shale.

In section 6, this unit consists of 11 m of sandstone with rare bioclasts. The nearby section 7 starts with coarse, lithic biocalcarenites containing about 20% unidentified, highly fractured bivalves and gastropods, grading towards the top into grey calcirudites with numerous basement crystals, and finally into yellowish, massive, well-cemented (bio)calcarenites with 5%–40% bioclasts.

The El Pimiento Member in section 8 consists of 6 m of medium- to coarse-grained biocalcarenites, in this case overlain with an erosional contact by the Punta Totoral Member.

In section 13, the El Pimiento Member has a non-conformable contact with Jurassic intrusives and forms a 21-m-thick, generally fining-upward succession of biocalcirudites, (bio)calcarenites, and minor sandstones with sparse bioclasts. In the basal biocalcirudites, which contain scattered, well-rounded basement clasts up to 10 cm in diameter, shell fragments make up to 70% of the rock, although whole *Ostrea* sp. also occur. The (bio)calcarenites are medium- to coarse-grained and contain between 10% and 80% bioclasts, as well as sub-angular to rounded basement clasts reaching 5 cm in diameter. Trace fossils include *Skolithos* and *Thalassinoides*.

Section 14 of Achurra (2004) is almost identical to section 13 of Henríquez (2006), but plots somewhat to the north of the latter according to the provided coordinates. The basal 20 m were considered by Achurra (2004) to belong to his unit 1. In addition to *Skolithos* and *Thalassinoides*, conical structures (Fig. 5) were observed, which are similar to those interpreted by Buck and Goldring (2003) as caused by the collapse of *Diplocraterion parallelum*, or by Howard et al. (1977) as due to the feeding activity of stingrays.

In section 16, the El Pimiento Member (unit 1 of Achurra, 2004) consists of 16 m of generally massive, but occasionally horizontally laminated biocalcarenites and biocalcirudites with scarce, reddish claystone lenses. Bioturbation is common, including tubes up to 40 cm long and 3 cm in diameter, probably made by arthropods. *Ostrea* and *Balanus* fossils occur near the base.

Section 21 shows about 5 m of coarse, bioturbated biocalcarenites overlying the basement, followed by 1.5 m of shale with slump structures and 7 m of sandstones largely devoid of shell fragments. Small paleochannels and rip-up clasts are present. This interval was considered by Achurra (2004) to belong to the basal part of his unit 2.

The benthonic foraminifer species *B. elegantissima*, *Pseudononion basispinatum*, and *B. pseudospissa*, as well as unidentified species of *Buccella*, *Hansenisca*, and *Cibides* were recorded within the El Pimiento Member. Planktonic foraminifers include *Globigerina bulloides* d´Orbigny 1826 and *Globigerina angustiumbilicata* Bolli 1957, as well as *Neogloboquadrina acostaensis* and *Neogloboquadrina pachyderma* Ehrenberg 1861 (Table 2).

Achurra (2004) obtained two $^{87}Sr/^{86}Sr$ ages of 10.3 ± 0.9 and 8.9 ± 1.0 Ma, respectively, from his unit 1. The samples were taken at the base and 20 m above the latter in section 14. Henríquez (2006), on the other hand, dated his unit 3 by $^{87}Sr/^{86}Sr$ at 10.4 ± 0.9 Ma. Based on the

**Fig. 5.** Conical trace fossils in the El Pimiento Member, attributed to the feeding activity of stingrays.

**Table 2**
Foraminifers identified in the Bahía Inglesa Formation, with maximum recorded water depths and age ranges indicated.

| |
|---|
| *Angulogerina angulosa*: <23.03 Ma |
| *Bolivina bicostata*: 326 m (max) |
| *Bolivina pseudospissa*: 0–326 m |
| *Bulimina marginata*: 809 m (max) < 5.33 Ma |
| *Buliminella elegantissima*: 354 m (max) |
| *Cassidulina laevigata*: 2,564 m (max) |
| *Globigerina angustiumbilicata*: 921 m (max) |
| *Globigerina bulloides*: 3,780 m (max); < 56 Ma |
| *Globigerina praebulloides*: 1,101 m (max); < 37.2 Ma |
| *Globigerinella calida*: 668–3,700 m |
| *Globigerinita glutinata*: 393–3,700 m |
| *Globigerinoides ruber*: 217 m (max) |
| *Globigerinoides trilobus*: 2,578 m (max) 23.0–1.81 Ma |
| *Globorotalia miocea conoidea*: 505 m (max) |
| *Globorotalia crassaformis*: 3,700 m (max) |
| *Globorotalia margaritae*: 6–809 m |
| *Globorotalia puncticulata*: 59–137 m |
| *Globorotalia scitula scitula*: 1–415 m |
| *Globorotalia tumida*: 2,578 m (max) |
| *Globorotaloides hexagonus*: 3,700 m (max) |
| *Gyroidina soldanii*: 515 m (max) |
| *Neogloboquadrina dutertrei dutertrei*: 438 m (max) |
| *Neogloboquadrina pachyderma pachyderma*: 106 m (max) |
| *Orbulina universa*: 3,700 m (max); < 15.97 Ma |
| *Pseudononion basispinatum*: 34–192 m |
| *Siphonodosaria advena*: 13.8–3.6 Ma |
| *Uvigerina subperegrina*: 330 m (max) |
| *Virgulinella pertusa*: 2–163 m |

overlapping error brackets, this would yield a range of 9.5–9.9 Ma for the El Pimiento Member, with a median age of 9.7 Ma.

### 3.2.2. Puerto Viejo Member (upper part of unit 1 and unit 2 of Achurra, 2004; unit 6 of Henríquez, 2006; unit 1 of Carreño, 2012)

The Puerto Viejo Member is composed of the upper part of unit 1 and the greater part of unit 2 of Achurra (2004) in sections 14 and 15, as well as unit 6 (in sections 4, 6, and 13, respectively), of Henríquez (2006). This predominantly fine-grained succession thins out towards the north.

In section 4, unit 6 of Henríquez (2006) consists of 4 m of yellowish, fine- to very fine-grained sandstones and siltstones. A sharp contact separates these beds from the overlying, buff shales and intercalated siltstones. Towards the top of this fining-upward succession is a 1-m-thick, intercalated silt- and claystone unit with contorted bedding, cut by small channels filled with mudstones. The Puerto Viejo Member is here capped by a thin shale unit with microcoquina lenses.

Section 6 shows 3 m of and shales and calcareous siltstones with very fine shell hash.

Section 13 consists of 6 m of reddish, bioturbated shales and fine-grained sandstones with occasional bioclasts, parallel lamination, high-angle planar cross-lamination, and rare ripple marks.

In section 14, the basal part of the Puerto Viejo Member was included by Achurra (2004) into the uppermost part of his unit 1, being composed of 3 m of medium- to fine-grained sandstones and shales. However, it overlies the El Pimiento Member as defined here with an erosional contact and is relatively free of bioclasts. The sandstones also show wave ripple marks and some bioturbation. The upper part, defined by Achurra (2004) as his unit 2, consists of 3 m of shales overlain by about 1 m of medium to fine sandstone.

The basal part of section 15 (Achurra, 2004) is composed of 10 m of finely laminated, bioturbated shales, which are here correlated with the upper part of the Puerto Viejo Member. Achurra (2004) included this succession in the basal part of his unit 2 at this locality.

In section 16, the Puerto Viejo Member is composed of 11 m of bioturbated, laminated shale with occasional slump structures.

The upper part of the Puerto Viejo Member in section 17 consists of about 8 m of fine to medium, horizontally bedded sandstone with *Thalassinoides* traces. This unit is eroded by small channels up to 10 m wide and 1–3.5 m deep, filled with thinly bedded, fine-grained yellow sandstone intercalated with reddish, sometimes highly contorted shales. The channel-fill occasionally drapes over the steep northern edges of the chutes. This section, measured by Le Roux (unpublished work) was considered by Carreño (2012) as her unit 1.

In section 21, the Puerto Viejo Member is composed of about 8 m of finely laminated shales.

The benthonic foraminifera of the Puerto Viejo Member include the *Bolivina* species *B. tumida* and *B. ticensis*, *Buliminella elegantissima*, *Pseudoparrella californica*, *Uvigerina subperegrina*, *Virgulinella pertusa* Reuss 1861, *Cassidulina laevigata* Cushman 1922, *Angulogerina angulosa* Williamson 1858, and unidentified species of *Pseudononion*, *Epistominella*, *Hoeglundia*, *Fursenkoina*, *Cibicides*, and *Globocassidulina*. Planktonic foraminifers observed are the *Globigerina* species *G. bulloides*, *G. angustiumbilicata*, and *G. praebulloides* Blow 1959, as well as *Globorotalia miocea conoidea*.

Although no direct dating has been done on the Puerto Viejo Member, its stratigraphic position suggests a range between 9.7 and 9.0 Ma, with a median age of 9.4 Ma.

### 3.2.3. Punta Totoral Member (upper part of unit 2, units 3 and 4 of Achurra, 2004; units 4 and 7 of Henríquez, 2006, basal part of unit 2 and 3 of Carreño, 2012)

This unit overlies the uppermost shales of the Puerto Viejo Member (unit 6 of Henríquez, 2006) with a sharp contact and crops out between Puerto Viejo and El Morro de Copiapó (Fig. 2). It consists of alternating biocalcarenites, biocalcirudites, and matrix-supported conglomerates showing mostly gradual upper and lower contacts. Although the great majority of bioclasts are highly fractured, some *Chlamys* specimens and unidentified gastropods have been preserved whole.

In section 2, the Punta Totoral Member is a 2-m-thick, clast-supported, medium to coarse conglomerate overlying biocalcarenites of the El Pimiento Member with an erosional contact. It was assigned by Henríquez (2006) to his unit 4. The clasts are polymictic, well rounded, poorly sorted, and vary in size between 1 and 25 cm. Well-developed imbrication is observed, and there is an absence of bioclasts. This bed is overlain with a sharp contact by about 2.5 m of fine to medium, massive calcarenites with scarce *Chlamys* fragments. Towards the top, these are overlain with an erosional contact by a 1-m-thick, polymictic, matrix-supported conglomerate with poorly sorted, rounded clasts varying from 1 to 20 cm in diameter. The matrix is composed of medium sand and fine shell hash. In turn, this conglomerate grades into 1.5 m of medium, parallel-laminated, as well as herringbone and high-angle planar cross-laminated sandstones intercalated with thin, well-cemented calcirudites, and fine conglomerates.

In sections 13 and 14, unit 3 of Achurra (2004) and unit 7 of Henríquez (2006) are 7 m thick and overlie the Puerto Viejo Member with a sharp contact. At the base, it has a 50-cm-thick, clast-supported conglomerate with well-rounded cobbles and boulders up to 50 cm in diameter, in turn overlain by a succession of medium- to coarse-grained biocalcarenites with thinner biocalcirudites and pebble-supported conglomerates. Some high-angle planar cross-bedding was recorded in the biocalcarenites and pectinoid fossils are present.

Section 15 shows about 16 m of interbedded fine to coarse sandstones with occasional ripple marks, bioturbated shales, thin, sometimes fining-upward, pebble-supported conglomerates with clasts up to 1 m in diameter, and a meter-scale biocalcirudite about 8 m from the base. This succession was included by Achurra (2004) in the upper part of his unit 2, but also encompassing his units 3 and 4. However, it has unifying lithological characteristics and is considered here to belong to the El Totoral Member.

In section 16, the Punta Totoral Member is represented by a 4-m-thick unit consisting of coarsening-up, fine to medium sandstones

overlain with an erosional contact by 2 m of polymictic, pebble-supported conglomerate. Some rip-up clasts are also present.

The basal part of unit 2 of Carreño (2012) in section 17, measured by Le Roux (unpublished work), consists of a 3.5 m thick, fining-upward succession grading from biocalcirudite at the base to medium-grained biocalcarenite. *Thalassinoides* and *Skolithos* traces are present in the basal, coarse-grained portion. It is here assigned to the Punta Totoral Member.

In section 18, the Punta Totoral Member (unit 3 of Carreño, 2012) is a 23-m-thick succession of interbedded conglomerates and medium to fine sandstones. It overlies the basement directly at this locality, showing a transitional zone in which well-rounded boulders and cobbles up to a few m in diameter occur in a matrix of weathered basement material. Some boulders protrude into the overlying, yellowish, pebbly to gritty, shelly sandstone. Bivalves, oysters, and barnacles were recorded. Higher up this sandstone becomes fine-grained and trough cross-laminated. A prominent conglomerate about 6 m from the base is up to 6 m thick, clast-supported and polymictic with well-rounded and sorted cobbles and boulders of sandstone, rhyolite, basalt, gabbro, and chert, most of which are probably derived from Mesozoic basement rocks such as the early Jurassic Caldera Gabbro (Godoy et al., 2003), as well as the Coastal Range to the east (Fig. 3). Most pebbles vary in size from 5 to 10 cm, but isolated gabbroic boulders reach up to 30 cm. A second, 6-m-thick conglomerate with channel features and trough cross-beds is present higher up, being underlain and overlain by fine- to very fine-grained sandstones with occasional trough cross-lamination and *Skolithos* traces.

Section 19 has 21 m of fine to coarse (slightly coarsening-upward) biocalcarenites with some well-preserved *Chlamys* sp., which erosionally overlie a 7.5-m-thick, polymictic, pebble-supported conglomerate attributed by Achurra (2004) to his unit 4. However, it is here reassigned to the Punta Totoral Member, which thus reaches its maximum recorded thickness of 28.5 m at this locality.

This member has a total exposed thickness of 16 m in section 20, where it overlies bioturbated, laminated shales of the Puerto Viejo Member. It has very fine to fine sandstones with minor shales in the basal 9 m, followed by calcarenites and calcirudites in the remainder of the profile.

In section 22, this member overlies the Jurassic basement, being composed of 7 m of biocalcirudites and matrix-supported conglomerates with angular clasts.

Benthonic foraminifers identified in the Punta Totoral Member include *Bulimina pyrula* d´Orbigny 1846, *Gyroidina soldanii* d´Orbigny 1826, *G. bulloides* d´Orbigny 1826, and *Siphonodosaria advena* Cushman and Laiming 1831.

A $^{87}Sr/^{86}Sr$ date of 9.0 ± 1.0 was obtained by Henríquez (2006) from shell fragments 4 m from the base of the Punta Totoral Member in section 14. In addition, Achurra (2004) reported a $^{87}Sr/^{86}Sr$ date for his unit 9 (section 15) of 9.2 ± 0.7 Ma, which here directly overlies the Punta Totoral Member. If his correlation of this biocalcirudite with the Caldera Beds is correct, this is clearly an aberrant age, as the latter is considered to belong to the Pleistocene. However, it is likely that the dated shell had been reworked from the underlying Punta Totoral Member, thus yielding an additional date for the latter. The two dates give a range of 10.0–8.0 Ma for this member, with a median age of 9.0 Ma.

### 3.2.4. Cerro Ballena Member (unit 8 of Carreño, 2012)

In section 32, a 9-m-thick succession of very fine to silty sandstones is exposed along a national road cut at Cerro Ballena. This outcrop, corresponding to unit 8 of Carreño (2012), has an extraordinarily well preserved vertebrate fossil record (Pyenson et al., 2014), including more than 40 large baleen whales (Balaenopteridae or rorquals), an extinct species of sperm whale (*Scaldicetus*), a walrus-like, toothed whale (*Odobenocetops* sp.), dolphins (Odontoceti), seals (Phocidae), and an aquatic sloth (*Thalassocnus natans*). Trace fossils include *Psilonichnus*, *Ophiomorpha*, and *Thalassinoides*, while apparent algal structures (small domes) are also preserved (Fig. 6).

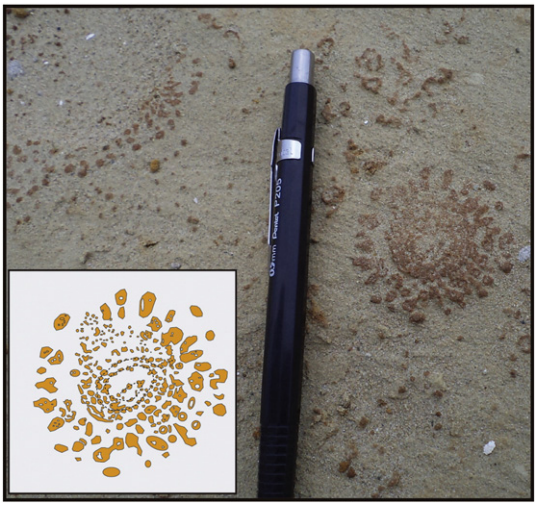

**Fig. 6.** Small domal structures in Cerro Ballena Member, attributed to algal filaments.

Although the lithostratigraphic correlation of this succession with other members is uncertain, Pyenson et al. (2014) assigned it an age of 9.03–6.45 Ma based on the species of aquatic sloth fossil (*T. natans*) and shark fossils (*Carcharodon hastalis*), which occur together in beds of this age in the Sacaco Basin of Peru. It is thus more or less time-equivalent with the La Higuera Member, which lies between the 9.0-Ma-old Punta Totoral Member and the 7.0-Ma-old Mina Fosforita Member. However, the supratidal flat environment of the Cerro Ballena Member is more compatible with the upper to middle shoreface environment of the Punta Totoral Member than with the outer shelf to upper continental slope environment of the La Higuera Member and parts of the Mina Fosforita Member. Therefore, it is considered to be slightly older than the La Higuera Member, with an age around 8.4 Ma.

### 3.2.5. La Higuera Member (unit 4 of Achurra, 2004; unit 8 of Henríquez, 2006; parts of units 2, 3, and 4 of Carreño, 2012)

This member is fairly easily recognizable, being dominated by poorly consolidated shales with many gypsum veins (Fig. 7) as well as intercalations of very fine-grained sandstones, siltstones, and diatomaceous clays. Both the shales and diatomaceous clays are finely laminated with a high content of fish scales.

Section 9 shows 23 m of shales with minor siltstones, usually less than 1 m thick, in unit 8 of Henríquez (2006).

**Fig. 7.** Gypsum veins in the La Higuera Member.

In section 16, 11 m of shales with rare, thin, very fine-grained sandstone beds and many cross-cutting gypsum veins are exposed. It was correlated by Achurra (2004) with his unit 4.

In section 17, the La Higuera Member consists of only 2.5 m of laminated siltstones and shales overlying the Punta Totoral Member, but it was evidently eroded by the Chorrillos Member along this part of the submarine canyon. It was attributed by Carreño (2012) to the upper part of her unit 2.

Section 18 has a similarly reduced thickness due to erosion along the submarine canyon, showing 3 m of horizontally bedded, fine-grained sandstones with slump structures and some *Skolithos* traces. This includes the upper portion of unit 3 of Carreño (2012).

The La Higuera Member reaches a thickness of at least 16 m in section 21, where it consists of shales with numerous gypsum veins. However, these shales overlie 3.5 m of fine-grained sandstones intercalated with shales, in turn resting on top of the 2.5 m thick Chorrillos Member. Below the latter are another 2 m of shales that might still belong to the La Higuera Member. If this is correct, the Punta Totoral Member is represented by only 0.5 m of conglomerate with shell fragments, which overlies about 8 m of shales forming part of the Puerto Viejo Member.

In section 22, 26 m of bioturbated, well-laminated shales with occasional very fine sandstone interbeds are present.

Benthonic foraminifers in the La Higuera Member include the *Bolivina* species *B. bicostata*, *B. pseudospissa*, and *B. sinuata* Galloway and Wissler, 1927, the *Buliminella* species *B.* cf. *elegantissima* and *B. peruviana*, as well as unidentified species of *Hoeglundia* and *Pseudononion*.

Based on stratigraphic and sedimentological considerations, the La Higuera Member is considered to be somewhat younger than the Cerro Ballena Member, i.e. at around 8.0 Ma.

*3.2.6. Chorrillos Member (basal part of unit 4 of Carreño, 2012, as based upon unpublished work of Le Roux)*

This member fills an at least 10-m-deep submarine canyon cutting from northeast to southwest into the La Higuera Member in sections 17, 18, and 21.

In section 17, occasionally imbricated basement pebbles and clast-supported rip-up clasts (up to 4 m long and 2 m thick), overlie a sharp, slightly irregular basal contact in chaotic fashion (Fig. 8). These rafts occur in all orientations from vertical to horizontal, although most are sub-parallel to the basal contact. There is a general coarsening-upward trend, with some boulders protruding into the overlying unit. This 4- to 5-m-thick bed is overlain with a sharp contact by 3 m of conglomerates with basement boulders up to 30 cm in diameter. Lenses of gritty, matrix to clast-supported conglomerate within these coarser conglomerates show horizontal lamination, trough-crossbedding and imbrication, with clasts dipping towards the east. The cobbles and boulders are well-rounded, without any clear size-grading. The Chorrillos Member is here overlain with a sharp contact by about 7 m of siltstones belonging to the Mina Fosforita Member.

In section 18, the Chorrillos Member is 3.5 m thick, filling a part of the submarine canyon that cuts into 3 m of fine-grained, laminated, bioturbated sandstone of the La Higuera Member. Here, it is a clast-supported conglomerate with dioritic boulders derived from the Mesozoic basement and angular to subrounded, very poorly sorted rip-up clasts than can exceed a meter in diameter. Along the steep, stepped northern edge of the channel, a sandstone rip-clast frozen in the process of being incorporated into this unit can be seen. At the top, the Chorrillos Member contains megaclasts protruding into the basal part of the Mina Fosforita Member. The underlying, fine-grained sandstone shows vertical fractures with cm-scale downward displacement on the channel side, indicating that the sandstone began to slump into the channel, which thus existed as such before deposition of the Chorrillos Member. Towards the north, the underlying sandstone thins out and steepens into the channel. The southern edge of the latter is more gradual, but in places shows conglomerate of the Chorrillos Member injected along the bedding planes of the underlying sandstone. Here, the channel-fill deposits are much finer, although they still contain some large boulders at the top.

The stratigraphic position of the Chorrillos Member suggests an age between that of the La Higuera Member and Mina Fosforita Members, i.e. 8.1 to 7.0 Ma, although in section 21 it appears to be emplaced within the former. Therefore, it is considered to be a time-equivalent of the La Higuera Member, but at least younger than its base. An age of around 7.5 Ma is proposed.

*3.2.7. Mina Fosforita Member (upper part of unit 4, unit 5 of Achurra, 2004; uppermost part of unit 8, as well as units 9 and 10 of Henríquez, 2006; units 4, 5 and 6 of Carreño, 2012)*

The Mina Fosforita Member is notably coarser than the La Higuera Member, being a generally fining-upward, reddish-brown succession of medium- to fine-grained sandstones, siltstones, and shales, with at least one fossil-rich, nodular phosphate bed (Fig. 9) and manganese nodules in its basal portion.

Section 9 shows, in the upper part of unit 8 of Henríquez (2006), that there are horizons with intensive bioturbation and abundant molds of *Turritella* and *Ostrea* spp. in the intercalated, very fine-grained sandstones and siltstones. A prominent, meter-thick phosphate-pebble conglomerate, attributed by Henríquez (2006) to his unit 9, occurs about

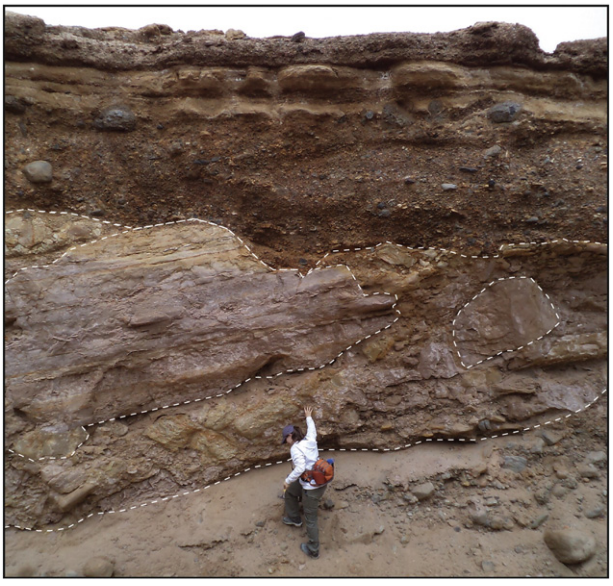

**Fig. 8.** Large blocks ripped up from the substrate in the Chorrillos Member.

**Fig. 9.** Nodular, fossil-bearing phosphate bed (middle of photo) in the Mina Fosforita Member.

10 m above the base of this member in this section, which has a total thickness of about 10 m. This lenticular unit overlies a local disconformity and contains angular, dense phosphate clasts in a fine to medium sandstone matrix. In this section, unit 10 of Henríquez (2006) is composed of siltstones and shales reaching a total thickness of 11 m.

In sections 10 and 11, unit 10 of Henríquez (2006) is characterized by fine-to medium-grained sandstones, occasionally slightly calcareous, with very thin siltstone and shale intercalations. In section 10, there are thin, well-consolidated, bioturbated sandstones with phosphate nodules and a prominent, grey sandstone with undetermined pelecypods and gastropods, *Turritella* and *Chlamys* fossils, as well as cetacean, seal, and penguin bones. Fish bones, scales, and teeth are also present. The trace fossils *Rosselia*, *Planolites*, *Ophiomorpha*, *Skolithos*, and *Monocriterion* were recognized in some intensively bioturbated horizons. Higher up in this unit, the sandstones are parallel-laminated with interbedded horizons showing climbing ripples. Some channel structures filled with contorted, fine-grained sandstone were observed (Fig. 10). Slump structures were also recorded in section 11.

In section 17, the Chorrillos Member, which fills a submarine canyon cut into in the upper part of the La Higuera Member, is succeeded by 6 m of siltstones with *Thalassinoides* traces, a thin phosphate-pebble conglomerate, a meter-thick, fine-grained sandstone, a thin conglomerate, and finally about 16 m of silty shales and shales with gypsum veins. Within the basal 12 m of this unit are manganese nodules described by Achurra et al. (2009).

In section 18, the upper part of unit 4 of Carreño (2012), which is here attributed to the Mina Fosforita Member, is dominated of about 11 m of very fine- to fine-grained, bioturbated sandstones with ripple marks, contorted bedding and dish structures, containing two polymictic conglomerates with basement clasts within the lowermost 5 m. The sandstones are overlain by a 1.5-m-thick phosphate-pebble conglomerate with borings (Fig. 6), in turn succeeded by 2.5 m of shale and 2 m of very fine-grained sandstone.

Section 22 shows 3 m of medium-grained biocalcarenites with pectinids and manganese nodules overlying the La Higuera Member with a sharp contact, followed by 2 m of polymictic conglomerates with angular clasts and manganese nodules. These are succeeded by 1.2 m of shale, a meter-thick monomictic "breccia" with angular basement clasts, and finally about 6 m of fine-grained, well-stratified sandstones.

Very fine-grained sandstone, siltstone, and shale with hematite and carbonate nodules form a 5-m-thick succession in section 23. Unidentified, branched trace fossils were also observed (Fig. 11).

In section 24, unit 5 of Achurra (2004) is composed of 15 m of very fine-grained to silty, bioturbated, horizontally laminated sandstones. They are brownish yellow to purplish grey and poorly consolidated.

In section 25, unit 5 of Carreño (2012) is composed of 2 m of biocalcarenites overlain by a meter-thick phosphate-nodule conglomerate containing basement clasts, shark teeth, vertebrate bones, and fish scales. Her succeeding unit 6 consists of 7.5 m of siltstones interrupted by a second, very thin phosphate bed about halfway up the sequence. Some slump structures, carbonate nodules, and unidentified traces are present above the latter.

**Fig. 10.** Channels filled with contorted, fine-grained sandstone in the Mina Fosforita Member.


**Fig. 11.** Unidentified trace fossils in the Mina Fosforita Member, possibly made by arthropods.

Section 26 shows 16 m of very fine- to fine-grained sandstones, containing two meter-thick biocalcirudites occurring below a fossiliferous phosphate-nodule bed about 7 m from the base. Shark teeth occur throughout the succession. Here and elsewhere in the phosphate bonebed, various fossils including seals (*Acrophoca* and *Piscophoca*), cartilaginous fishes, cetaceans, sloths, and rats, have been found (Walsh and Hume, 2001; Walsh and Naish, 2002).

Unit 6 of Carreño (2012) in section 27 consists of two thin (less than 1 m) phosphate beds separated by an equally thin shale bed at the base, with the lower phosphate containing vertebrate bones and shark teeth. This is overlain by about 6 m of very fine-grained sandstones grading upward into siltstones, containing a thin volcanic ash bed at the top.

Section 28 is composed of 12 m of shales and siltstones with occasional, very fine-grained sandstones, but a meter-thick phosphate bed with vertebrate bones and shark teeth occurs at the base of the exposure. $Fe_2O_3$ and $CaCO_3$ nodules are present throughout the succession.

The benthonic foraminifers *Bulimina marginata* d´Orbigny 1826, *B. elegantissima*, *P. basispinatum*, as well as the *Bolivina* species *B. bicostata* and *B. pseudospissa*, were identified in the Mina Fosforita Member. The only planktonic species identified is *N. pachyderma*.

K–Ar dating of an ash layer cropping out about 7 m above the basal phospatic bonebed at Bahía Inglesa indicated an age of 7.6 ± 1.3 Ma (Godoy et al., 2003). Henríquez (2006), on the other hand, obtained a $^{87}Sr/^{86}Sr$ date of 6.8 ± 0.8 Ma from his unit 10. The overlapping error brackets yield a range of range 6.3–7.6 Ma, with a mean age of 7.0 Ma. This contradicts the maximum recorded age for *B. marginata* of 5.33 Ma (Encyclopedia of Life: http://eol.org/pages/490131/overview). However, fossil teeth of the lamnid shark *Carcharodon hastalis* (Suárez y Marquardt, 2013) and *C. hubbeli* in the phosphatic bonebed also support a late Miocene age, the latter species in fact suggesting an age between 6 and 8 Ma (Ehret et al., 2012). This means that the established age range of *B. marginata* should be revised.

*3.2.8. Rocas Negras Member (unit 6 of Achurra, 2004; unit 12 of Henríquez, 2006; unit 7 of Carreño, 2012)*

This member occurs in an isolated outcrop in section 8, where unit 12 of Henríquez (2006) overlies calcirudites and calcarenites of the El Pimiento Member with an erosional contact. The basal part contains well-rounded clasts of Jurassic to early Cretaceous basaltic andesite up to 20 cm in diameter, probably derived from the Coastal Range (Fig. 3), followed by well-cemented, sandy calcirudites containing *Turritella*, *Chlamys*, and *Ostrea* sp. Hummocky-and-swaley cross-lamination was recorded in this bed, which is about 1 m thick at this locality.

In section 24, unit 5 of Achurra (2004) is succeeded after a 2 m covered interval by 8 m of medium-grained calcarenites with occasional trough cross-lamination and oyster fossils, attributed to his unit 6.

In section 25, the Mina Fosforita Member is overlain with an erosional contact by about 5 m of biocalcirudites arranged in fining-upward units, considered by Carreño (2012) as her unit 7, but here designated to the Rocas Negras Member. These contain abundant basement clasts, bivalves and *Ostrea* sp. A meter-thick tuffaceous bed is present near the base.

Section 26 is an identical section to that at section 25, with unit 6 of Achurra (2004) composed of 5 m of biocalcarenites showing bioturbation, occasional trough cross-bedding, pectinoids, and oysters.

The Rocas Negras Member attains its maximum recorded thickness in section 29, where unit 6 of Achurra (2004) is a 30 m succession dominated by medium- to very coarse-grained biocalcarenites and biocalcirudites, with monomyctic conglomerate, fine-grained sandstone, and shale in the basal 7 m.

This unit yielded the following benthonic foraminifers: the *Bolivina* species *B. bicostata* and *B. pseudospissa*, *Bulimina marginata*, *Buliminella elegantissima*, *P. basispinatum*, and unidentified *Pseudononion* and *Neoeponides* spp. The planktonic representatives include *G. bulloides*, *Globigerinoides trilobus* Reuss, the four *Globorotalia* species mentioned below, as well as *N. pachyderma*.

The Rocas Negras Member was dated by $^{87}Sr/^{86}Sr$ on a well-preserved gastropod at 4.9 ± 0.7 Ma (Henríquez, 2006), while three $^{87}Sr/^{86}Sr$ dates of 4.6 ± 0.5, 4.4 ± 0.5, and 3.7 ± 0.5, respectively, were also obtained from this member by Achurra (2004). The presence of *B. marginata* suggests an age of less than 5.33 Ma (Encyclopedia of Life: http://eol.org/pages/490131/overview), while the coincident occurrence of *Globorotalia tumida* Brady, *G. margaritae* Bolli and Bermudez 1965, *G. puncticulata*, and *G. crassaformis*, as well as vertebrate fossils also confirm a Pliocene age (Srinivasan and Kennett, 1981; Valenzuela-Toro et al., 2013). The overlapping age brackets of the four Sr dates indicate a mean age of 4.2 Ma.

*3.2.9. Quebrada Blanca Member (units 7, 8 and 9 of Achurra, 2004; unit 11 of Henríquez, 2006)*

This member is highly variable and because its sections are far apart, correlation between them is uncertain. In section 12, it is a poorly consolidated unit with a thin, matrix-supported, small-pebble conglomerate at the base that contains rounded clasts as well as fractured shells. It grades into about 3.5 m of fine to medium, finely laminated sandstones with thin conglomerate interbeds, as well as calcirudites showing low-angle planar cross-lamination.

In section 30, about 7 m of very fine sandstones and shales correspond to the basal, fine-grained part of the Quebrada Blanca Member, here overlain by 1.5 m of very fine- to fine-grained sandstones interbedded with thin, polymictic, clast-supported conglomerates containing angular to rounded phosphate pebbles, chaotic rip-up clasts (Fig. 12) and cetacean bones. These are followed by 3 m of coarse biocalcirudites with thin sandstone lenses, trough cross-bedding, and some phosphate nodules.

Section 31 shows a 23-m-thick succession dominated by yellowish white, diatomaceous shales, but with two 2- to 3-m-thick, shell-rich conglomerates near the base and at the top. About 7 m from the base

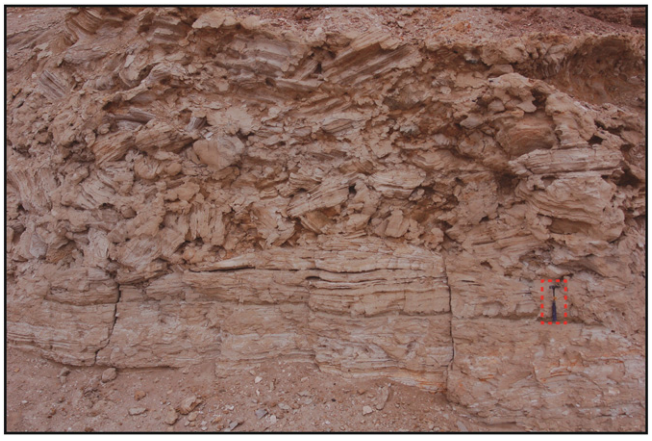

**Fig. 12.** Chaotic rip-up clasts in the Quebrada Blanca Member attributed to a tsunami backflow event.

is also a 2-m-thick conglomerate formed by substrate rip-clasts, which grades into a meter-thick calcirudite. Shark teeth were found in this bed.

Unidentified species of *Neoeponides* and *Hansenisca* were reported from the Quebrada Blanca Member by Henríquez (2006), while Achurra (2004) identified the *Neogloboquadrina* species *N. pachyderma* and *N. dutertrei* d´Orbigny 1839, the *Globigerinoides* species *G. ruber* d´Orbigny 1839 and *G. trilobus*, the *Globorotalia* species *G. scitula* Brady 1884 and *G. tumida*, *Globigerinella calida*, *Globigerinita glutinata*, *Globorotaloides hexagonus*, and *Orbitulina universa*.

Achurra (2004) obtained a $^{87}Sr/^{86}Sr$ date of 2.4 ± 0.5 Ma for the basal part of the Quebrada Member in section 30. The only other age indication is the presence of *Neogloboquadrina dutertrei* recorded in his unit 8. This foraminifer first appeared in the *Globorotalia margaritae margaritae* subzone (N18), i.e. at the base of the Pliocene at 5.3 Ma (Bolli et al., 1985).

## 4. Environmental interpretation of the different units

### *4.1. Angostura Formation*

The Angostura Formation only occurs in and around the present Copiapó River mouth, grading into the typical fluvial gravels of the Angostura Gravel Formation upstream (Godoy et al., 2003). The red colour of the conglomerates may be due to either prolonged weathering of the hinterland rocks that provided many of the clasts, or to partially oxidizing conditions of deposition, as for example on longitudinal bars. Horizontal, upper flow regime stratification suggests fast currents, as supported by small channels filled with broken shell fragments, whereas the presence of *Balanus*, *Ostrea*, and *Chlamys* sp. indicates a shallow marine environment with some freshwater input. The benthonic *Bolivina* species *B. bicostata* and *B. pseudospissa*, as well as *B. elegantissima*, have maximum recorded depth ranges of less than about 350 m (Gross, 2001; Encyclopedia of Life: http://eol.org/pages/488101/overview; http://eol.org/pages/6841343/overview; http://eol.org/pages/6999360/overview), but all three species also occur in the upper shoreface environment. Biocalcirudite beds or lenses were probably deposited on local shoals. This member therefore represents a relatively high-energy river-mouth environment, i.e. fluvially dominated estuarine conditions with clear marine interaction.

### *4.2. Bahía Inglesa Formation*

#### *4.2.1. El Pimiento Member*

This member is dominated by biocalcirudites and biocalcarenites with broken *Ostrea*, *Balanus* and *Chlamys* fragments, indicating high-energy conditions such as marine shoals affected by turbulent wave action, which is supported by the presence of *Skolithos* traces. The

polymictic conglomerate in section 4 contains large granitoid clasts probably derived from the Morro Copiapó Granodiorite, which crops out sporadically throughout the study area (Fig. 2). This suggests subaerial exposure and erosion of the latter in a rocky shoreline environment. Well-developed imbrication indicates strong offshore-directed rip currents. However, the combined presence of low- and high-angle cross-lamination in the overlying sandstones signals the existence of ridges and runnels in an upper shoreface environment, so that the beach changed from a reflecting to dispersive type. On the other hand, well-preserved, articulated *Chlamys* sp. have also been found in life position in calcarenites of this member (Henríquez, 2006), suggesting more tranquil local conditions, perhaps in depressions between shoals or in a somewhat deeper, lower shoreface environments. Such deeper water conditions at greater distances from the coastline could explain the presence of *Thalassinoides* traces (Buatois et al., 2002), as well as sandstones devoid of shell fragments, shales, and claystone lenses occurring within small paleochannels. The El Pimiento Member is therefore attributed to a mainly upper shoreface environment in the vicinity of freshwater creeks, but with sea-level oscillations causing temporary middle to lower shoreface conditions. The latter is supported by the presence of the benthonic foraminifer *P. basispinatum*, which has been recorded in a depth range of 34–192 m (Culver and Buzas, 1980; Nomura, 1982; Encyclopedia of Life: http://eol.org/pages/6815614/overview).

#### 4.2.2. Puerto Viejo Member

The generally fining-upward succession of the Puerto Viejo Member reflects a marine transgression. The fine- to medium-grained sandstones intercalated with shales are attributed to a middle–lower shoreface environment, as supported by *Thalassinoides* and *Skolithos* traces that according to Buatois et al. (2002) are more typical of the middle than the upper shoreface. The fact that they are locally cut by small channels filled with thinly bedded sandstones and shales suggests the existence of hyperpycnal flows transporting sand and mud into the offshore environment. This is supported by abundant climbing ripples, indicating a high suspension load, and a relatively high gradient exceeding 1°, as suggested by slump structures (Camacho et al., 2002).

The benthonic foraminifer species *B. bicostata*, *B. pseudospissa*, *B. elegantissima*, and *U. subperegrina* suggest water depths of less than 330 m (Gross, 2001; Encyclopedia of Life: http://eol.org/pages/488101/overview; http://eol.org/pages/6841343/overview; http://eol.org/pages/6999360/overview; http://www.eol.org/pages/6816852/overview), whereas *V. pertusa* has only been recorded in depths up to 163 m (Hayward, 2015; Encyclopedia of Life: http://www.eol.org/pages/489938/overview), but occurs mainly in water depths less than 60 m (Nigam and Anantha Padmanabha Setty, 1982). This supports a middle to lower shoreface environment.

#### 4.2.3. Punta Totoral Member

The facies of the Punta Totoral Member are similar to those of the El Pimiento Member and parts of the Puerto Viejo Member. Pebble-supported conglomerates with large basement boulders and bivalves, oysters and barnacles reflect a rocky coastline receiving some freshwater input from local creeks. The biocalcirudites were probably deposited on high-energy shoals in an upper shoreface environment, as supported by the presence of *Skolithos* traces. On the other hand, planar and herringbone cross-laminated calcarenites with whole *Chlamys* and gastropod specimens suggest a quieter, upper shoreface environment with ridges and runnels under the influence of tidal currents. Bioturbated shales interbedded with fine- to coarse-grained, ripple-marked sandstones correspond to a middle shoreface environment, as also signalled by the presence of *Thalassinoides* traces. All these facies occur in different stratigraphic positions within the Punta Totoral Member, suggesting rapid sea-level oscillations in contrast to the more general marine transgression reflected by the Puerto Viejo Member.

#### 4.2.4. Cerro Ballena Member

The depositional environment of the Cerro Ballena Member was interpreted by Pyenson et al. (2014) as a supratidal flat due to the presence of wave ripple lamination, *Thalassinoides*, *Ophiomorpha*, and *Psilonichnus* traces, as well as small, domal algal structures. An 80-cm-thick bed at the top of the measured section showing low-angle planar cross-lamination suggests a beach environment and probably formed on a barrier bar that protected the supratidal flat from the open ocean to the west. This is suggested by the presence of E-W orientated wave ripples lower down in the profile, which indicates that waves did not reach the tidal flat from the west, but propagated from the south under the influence of the prevailing northerly winds. Using the distance from the nearest basement outcrops to the south, assumed to have formed the shoreline of an embayment or estuary south of the outcrops, the mean sandstone grain size, and normal wind conditions during storms, a water depth of about 1.5 m was calculated, enough to allow the carcasses of large whales and other vertebrates to float in from the south (Pyenson et al., 2014).

#### 4.2.5. La Higuera Member

This member is dominated by bioturbated shales, often with cross-cutting gypsum veins, but also showing very fine to fine sandstones. The sometimes intensive bioturbation and local, high concentrations of fish scales within the shales, suggest that the La Higuera Member was deposited very slowly, which would be typical of an outermost shelf to upper continental slope environment during a relative sea-level highstand. Slump structures encountered in this member would be consistent with the higher gradients of the upper continental slope. Outermost shelf to uppermost continental slope depths are also supported by the benthonic foraminifers *B. bicostata*, *B. pseudospissa*, *B. elegantissima* (Encyclopedia of Life: http://eol.org/pages/488101/overview; http://eol.org/pages/6841343/overview; http://eol.org/pages/6999360/overview), and *Bolivina sinuata* (Galloway and Wissler, 1927), whereas *B. pyrula*, *G. soldanii*, and *S. advena* typically occur in depths exceeding 500 m (Ingle et al., 1980).

#### 4.2.6. Chorrillos Member

The location of this member within a relatively large submarine canyon eroded into the Higuera Member, together with a general coarsening-upward trend, indicate a large debris flow from the east. That the canyon already existed before this event is shown by synsedimentary faults in the underlying sandstones indicating slumping into the channel, as well as the fact that the dip of these sandstones steepens as they enter the northern flank of the canyon. The presence of gravelly sills injected from the base of this flow along the bedding planes of the underlying unit, as well as clasts several meters in diameter ripped up from the substrate, are features typical of tsunami backflow events (e.g. Le Roux et al., 2004, 2008; Le Roux, 2015).

#### 4.2.7. Mina Fosforita Member

The Mina Fosforita Member shows the highest variability in depositional environments of the Bahía Inglesa Formation, varying from the upper shoreface to upper continental slope. Scarce poly- and monomictic conglomerates and intensively bioturbated beds with *Turritella* and *Ostrea* molds suggest short-lived upper shoreface conditions with some freshwater influence. Some of the conglomerates have angular clasts and possibly formed by cliff collapse in a rocky shoreline environment. Medium-grained biocalcarenites and bioturbated, fine- to medium sandstones interbedded with shales, on the other hand, are similar to parts of the Totoral Member and therefore also attributed to a middle shoreface environment. This is supported by the trace fossil assemblage represented by *Rosselia*, *Planolites*, *Ophiomorpha*, *Skolithos*, and *Monocriterion* (Buatois et al., 2002).

Phosphatic conglomerates associated with siltstones containing *Thalassinoides* traces are more typical of the lower shoreface or continental shelf. According to the classification of Garrison (1992), the

Bahía Inglesa phosphates are of the types P and D, the former being commonly transformed to the latter due to cementation with carbonate fluorapatite, forming hardgrounds and nodules. Blatt et al. (1972) postulated that phosphates of this type typically precipitate in water depths between 45 and 180 m during the upwelling of cold, deep ocean water rich in phosphates and other nutrients. Trough cross-lamination and small channels filled with contorted, fine-grained sandstone, associated with sandstones showing climbing ripples, could indicate hyperpycnal flow events, which normally occur close to river mouths.

Despite the fact that most of the avifauna comprise species typically dwelling far from land, the fossil record also includes sulids and juvenile spheniscids (penguins) indicating an environment closer to the shore (Chavez, 2008). Some fossil chondrichthyan fishes suggest water depths of up to 200 m (Walsh and Hume, 2001). The benthonic foraminifer species *B. bicostata* and *B. pseudospissa*, as well as *B. elegantissima* and *P. basispinatum*, are typically found on the continental shelf (Encyclopedia of Life: http://eol.org/pages/488101/overview; http://eol.org/pages/6841343/overview; http://eol.org/pages/6999360/overview; http://eol.org/pages/6815614/overview), although *B. marginata* has been recorded to a maximum depth of 809 m (Encyclopedia of Life: http://eol.org/pages/490131/overview).

In the Mina Fosforita Member, slow deposition is suggested by the relative abundance of shark teeth and cetaceous bones in thick, clay-rich sandstone successions. The fining-upward biocalcirudite beds in these units could represent storm events that eroded nearshore shoals and redistributed the material over the continental shelf. However, in the manganese nodule-bearing shales, the presence of *C. laevigata* suggests water depths between 200 and up to 2,564 m (Achurra et al., 2009; Polovodova Asteman and Nordberg, 2013; Encyclopedia of Life: http://eol.org/pages/488135/overview), although *B. sinuata* has a maximum recorded depth of 326 m (Encyclopedia of Life: http://eol.org/pages/6999376/overview). Therefore, uppermost continental slope conditions can also be assumed. The presence of gypsum veins in these shales was attributed by Achurra et al. (2009) to the upwelling of cold, nutrient-enriched waters supporting a large population of plankton, which consumed oxygen and created a belt of anaerobic sedimentation on the continental slope following their death and decomposition. Anaerobic bacteria thus reduced $SO_4$ dissolved in the seawater and formed $H_2S$ that reacted with iron minerals in the sediment to precipitate FeS. This low pH, strongly reducing environment became saturated with calcium obtained by the dissolution of calcareous organisms and precipitated gypsum when the product of the calcium and $SO_4$ concentrations exceeded the gypsum solubility product. This interpretation was based on a similar situation on the present Namibian continental slope described by Siesser and Rogers (1976).

#### 4.2.8. Rocas Negras Member

The dominance of biocalcirudites and biocalcarenites in this member suggests an upper to middle shoreface environment, although the fining-upward biocalcirudites with basement clasts were evidently deposited as tempestites or storm beds on the lower shoreface. This is supported by the presence of hummocky and swaley cross-lamination, whereas *Turritella*, *Chlamys* and *Ostrea* species in these beds can be attributed to their erosion from shallow water areas by the storm waves.

#### 4.2.9. Quebrada Blanca Member

This member is of variable composition, but the presence of (bio)calcirudites showing low-angle planar and trough cross-lamination indicates strong rip currents and wave action, probably on partly emergent shoals in an upper shoreface environment. Conglomerates with rounded clasts rich in fractured shells could also indicate local beaches. The thick, diatomaceous shale-dominated unit indicates a return to deeper water, possibly an outer shelf environment, whereas the conglomerate with large substrate rip-up clasts represents a second, younger tsunami event.

## 5. Relative sea-level changes as related to tectonic uplift and subsidence

The sedimentary facies and stratigraphic succession of the Bahía Inglesa Formation reflect sea-level oscillations that can be used, in conjunction with published global sea-level curves (Hardenbol et al., 1998), to deduct relative tectonic movements affecting this part of the southeastern Pacific coastline during the Neogene. The methodology, known as geohistory analysis (Van Hinte, 1978), consists of determining the age and depositional depths of the units composing a stratigraphic succession, relating the paleobathymetry to the global sea level at the time, and calculating the progressive elevation of a reference surface relative to the present sea level. The mean cumulative thickness of the units is generally employed, but in this case, the thicknesses of the different members are highly variable from section to section and in some cases incomplete, e.g. where the base or top of the member was not exposed. Therefore, the maximum measured thickness of each particular member, rounded to the nearest meter, was considered to be more representative. This was also the procedure followed at Carrizalillo and Tongoy further south, making the different curves in Fig. 13 compatible. The cumulative maximum thickness was measured upward from the reference surface (the contact between the Angostura Formation and the Jurassic basement at Puerto Viejo) to the middle of each member, progressively adding the maximum thickness of each member to those of the underlying members. The Chorrillos Member was left out in this case, as it occupies a submarine valley cutting at least 10 m into the La Higuera Member and is thus not representative of the general environment. However, it might indicate a short pulse of uplift and subaerial exposure prior to its deposition. As concerns the paleobathymetry, the following mean depositional depths were assigned to the different facies: supratidal flat, 1 m; foreshore, 0 m; estuary, −10 m; upper shoreface, −20 m; middle shoreface, −50 m; lower shoreface, −80 m; inner shelf, −120 m; outer shelf, −170 m; upper continental slope, −380 m. Where a particular member was deposited in a range of environments, the mean depth was calculated as follows, e.g. upper shoreface — inner shelf: $\frac{(-20)+(120)}{2} = -70\text{m}$. Table 3 and Fig. 13a show the results of this analysis.

In Fig. 13a, the individual data points linked by a fine stippled line represent a detailed, but possibly less accurate rendering of the basement behavior during the Tertiary, whereas the thick, continuous line is considered to better reflect major, more representative changes in the latter. It is thus more directly comparable with the basement behavior at Carrizalillo (Figs. 1, 13b, 14) and Tongoy (Figs. 1, 13c, 14) further to the south (Le Roux et al., 2005a,b).

## 6. Discussion

Correlation between the different units in the Caldera Basin is difficult due to rapid lateral facies changes and the fact that very similar environments, mostly ranging from the upper to lower shoreface, occurred repeatedly due to sea-level oscillations combined with tectonic movements. This is complicated by the fact that most of the members locally overlie the basement directly, which indicates a very irregular topography sculptured by subaerial erosion before deposition of the Bahía Inglesa Formation. Nevertheless, a few important trends do emerge.

The absence of rocks with an age between 15.3 and 10.4 Ma in the coastal sector between Puerto Viejo and Caldera indicates a major unconformity, suggesting that this part of the coastline was subjected to subaerial erosion from the Langhian to early Tortonian. The irregular topography also indicates that there was no period of tectonic and/or sea-level stability to allow peneplanation of the coastal sector.

The Angostura Formation was deposited in a shoreline environment, probably a paleo-estuary of the Copiapó River, but at an elevation of more than 100 m above present sea level according to global sea-level curves. Starting sometime after 15.3 Ma, tectonic subsidence occurred simultaneously with a drop in global sea level but was outpaced by

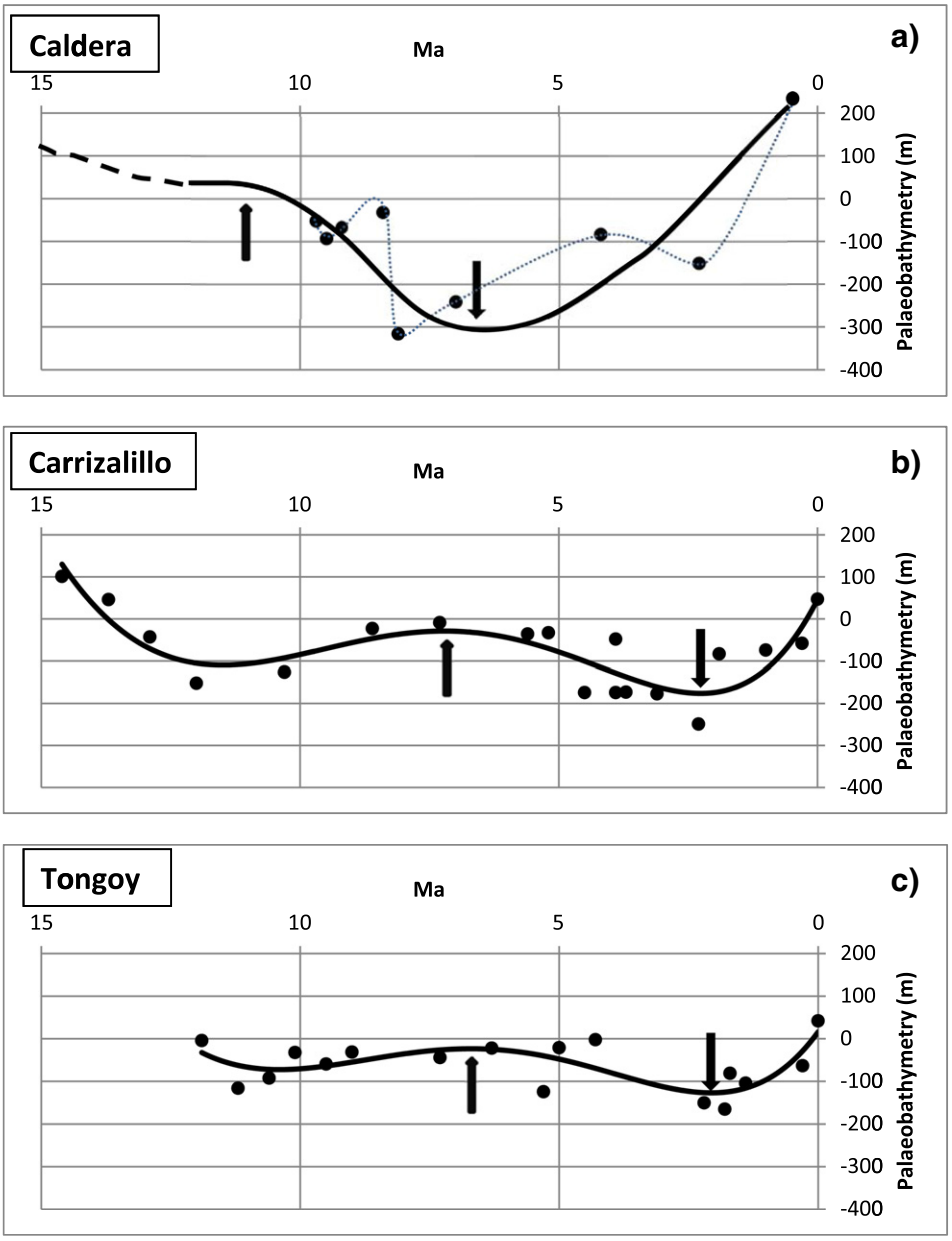


**Fig. 13.** Relative elevation of the basement of the Bahía Inglesa Formation with respect to present-day sea level during the Miocene, as based on geohistory analysis. Tectonic movements in the Carrizalillo and Tongoy Basins repeat the same uplift–subsidence–uplift patterns, but are more subdued.

the latter, so that the irregular, subaerial topography persisted. Le Roux et al. (2005a,b, 2006) recorded a period of coastal subsidence in the Coquimbo Basin of south central Chile between about 15 Ma and 11 Ma, which also coincided with a change from estuarine peat swamp conditions to deep marine embayments in the Valdivia and Osorno Basins (Fig. 1) (Elgueta et al., 2000; Le Roux and Elgueta, 2000). In the Caldera Basin, no marine deposition is recorded until about 10.4 Ma. However, from before this moment in time to around

**Table 3**
Data used for geohistory analysis of the Bahía Inglesa Formation.

| Formation/Member | Mean age (Ma) | Cumulative thickness (m) | Global sea level (m) | Depositional environment | Paleobathymetry (m) | Reference surface (m) |
|---|---|---|---|---|---|---|
| Angostura | 15.3 | 4 | 130 | Estuary | −10 | 116 |
| El Pimiento | 9.7 | 16 | −1 | Upper–middle shoreface | −35 | −52 |
| Puerto Viejo | 9.4 | 22 | −1 | Upper shoreface–inner shelf | −70 | −93 |
| Punta Totoral | 9.0 | 33 | 1 | Upper–middle shoreface | −35 | −67 |
| Cerro Ballena | 8.4 | 38 | 5 | Supratidal flat | +1 | −32 |
| La Higuera | 8.0 | 51 | 10 | Outer shelf–upper continental slope | −275 | −316 |
| Mina Fosforita | 7.0 | 62 | 21 | Upper shoreface–upper continental slope | −200 | −241 |
| Rocas Negras | 4.2 | 77 | 29 | Upper–middle shoreface | −35 | −83 |
| Quebrada Blanca | 2.4 | 98 | −3 | Upper–lower shoreface | −50 | −151 |

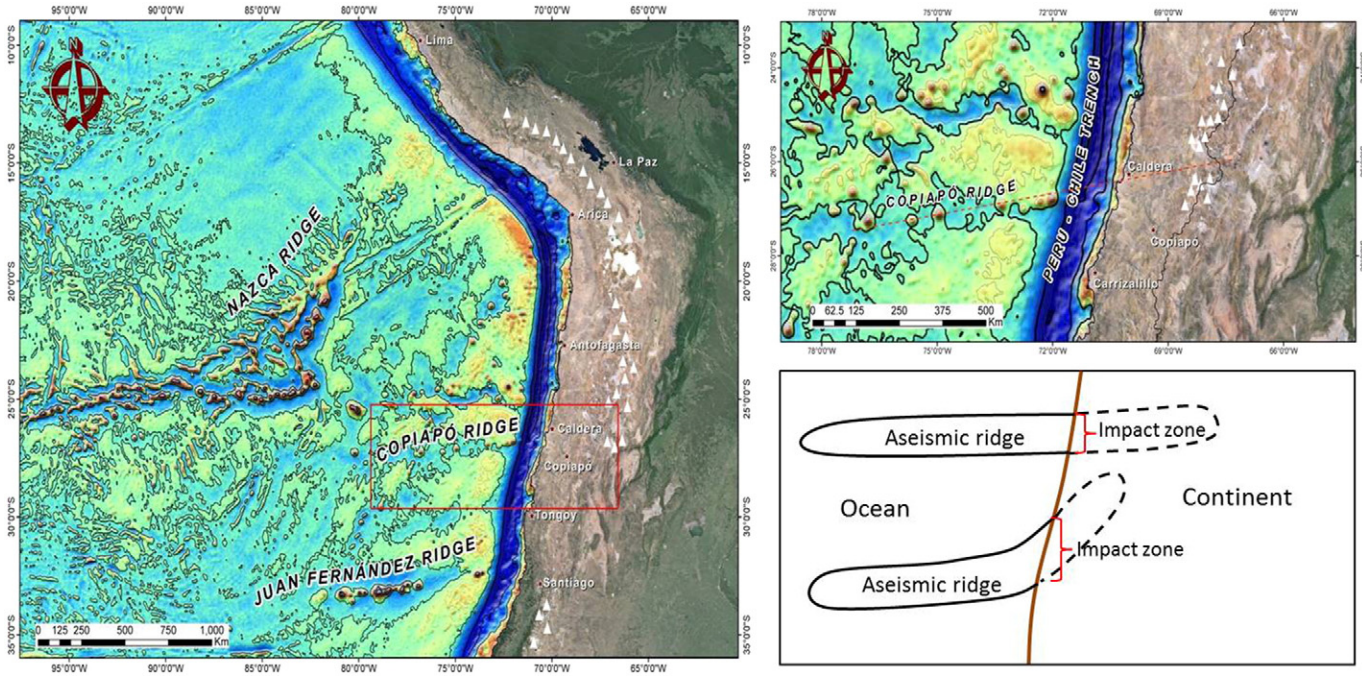


**Fig. 14.** (a) Present positions of Nazca, Copiapó, and Juan Fernándes Ridges. White triangles show active volcanoes. Note how present axes of Nazca and Juan Fernández Ridges deviate towards the left as they approach the edge of the continent. (b) Inset (corresponding to red square in a) shows gap in volcanism coinciding with projection of Copiapó Ridge below the continental crust. (c) Schematic figure shows how angle of ridge incidence affects impact area. With a high angle of incidence (above) impact area (red bracket) is smaller but more intense. As incidence angle decreases (below) due to oroclinal bending, impact zone increases but becomes less intense.

5.65 Ma, the basin continued to subside, reaching nearly 350 m below present sea level and bringing the depositional depth to that of the upper continental slope. This contrasts with the elevation history of the central Andes Range. Gregory-Wodziki (2000) maintained that the Altiplano of the central Andes had attained no more than half its modern elevation by 10.7 Ma, and that surface uplift of 2,300–3,400 m occurred since the late Miocene. Bissig et al. (2002) also recognized an important erosional surface in the high central Andes that formed in the interval 10–6 Ma. Further south in the Navidad Basin (Fig. 1), Gutiérrez et al. (2013) concluded that marine regression and tectonic uplift started soon after 11 Ma. Therefore, some tectonic process must have led to subsidence of the Caldera Basin while the Andean hinterland was rising and coastal uplift was occurring further south. This is here attributed to southward migration of the Juan Fernández Ridge (JFR), causing this part of the continental crust to first rise and then subside to fill the mantle void left in its wake.

Yañez et al. (2001) showed the location of the NW-striking continuation of the JFR more or less opposite Caldera at 12 Ma, which would constrain the beginning of subsidence to around 11 Ma. According to these authors, the migrating ridge reached the Navidad area (Fig. 1) 770 km further to the south at about 10 Ma, which would imply a migration rate of 38.5 cm per year. This portion of the ridge becoming parallel to the relative direction of plate movement at this time, it did not migrate further south after 10 Ma. However, Kay and Abbruzzi (1996) considered that the JFR reached this configuration only between 5 and 3 Ma, which in this case would imply a mean migration rate of 9.6 cm per year.

The present Copiapó Ridge (Fig. 14) opposite Caldera is causing similar crustal doming and thickening where it intercepts the trench, as shown by Álvarez et al. (2015). Using the Earth Gravitational Model to calculate the gravity anomaly and vertical gravity gradient in the central Andes region opposite this aseismic ridge, these authors propose that there is a spatial relationship between its projected subduction and neotectonic deformation associated with volcanic eruptions along the Ojos del Salado–San Buenaventura volcanic lineament. However, it should be noted that there is a gap in active volcanism just to the north of their ridge projection, which might be an alternative location for the latter if it is deflected slightly towards the north (Fig. 14). This seems to make more sense, because crustal thickening should lead to a cessation of volcanism as presently observed over the flat-slab zone. Nur and Avraham (1981), for example, proposed that the assimilation of aseismic ridges along the South American coastline could explain the lack of volcanic activity along these parts of the Andes. In this regard it is interesting that the initial subsidence of the Caldera Basin between 11 and 10 Ma coincided with volcanic eruptions leading to the large Copiapó Ignimbrite in the volcanic arc directly to the east (Mpodozis et al., 1995), i.e. volcanism occurred only after the ridge started to migrate away from this area. This might be attributed to mantle-deep faults generated by extensional stress in the subsiding crust.

The individual data points in Fig. 13 (fine stippled line) show a possible interruption in the subduction trend of the Caldera Basin that caused uplift of about 75 m during the period 9.7–8.3 Ma, followed by very rapid subsidence of nearly 300 m from 8.3 to 8.1 Ma. The submarine canyon in which the Chorrillos Member was deposited at about 7.5 Ma predates this age (see Section 4.2.6.), and might possibly have formed sub-aerially during this short-lived pulse of uplift. The latter could have been due to a topographic outlier of the JFR, as can be seen along the present ridge where anomalous peaks occur up to 30 km from the ridge axis. The time from 9.7 to 8.3 Ma also coincides with a gap in the eruption of the Copiapó Ignimbrites (Mpodozis et al., 1995), which would reinforce the idea of reduced volcanism during the presence of aseismic ridges or their outliers below the continental crust.

In spite of the possible correlation between this pulse of uplift, the submarine canyon at Chorrillos, and temporary cessation of the Copiapó volcanism, this event is considered to be somewhat anomalous and implies a very rapid subsidence rate of 1.5 mm/year. Therefore, the more general interpretation is preferred in Fig. 13 (thick solid line), which indicates continual subsidence at a rate of 0.06 mm/year from 11 to 5.65 Ma. At this point, a dramatic turnaround uplifted the basin by at least 250 m. In the coastal sectors further south, similarly strong uplift commenced at around 2.3 Ma (Le Roux et al., 2005a,b, 2006). This

period coincides with the Messinian–Pliocene Warming episode between 6 and 2.8 Ma (Le Roux, 2012), linked to an increase in the East and South Pacific Rise spreading rates (Rea, 1976; Cande and Leslie, 1986; Le Roux et al., 2005a), and uplift of the Bolivian Orocline (Ghosh et al., 2006). At 6 Ma, the volcanic arc front was also displaced eastward, which can be linked to crustal thickening during back-arc thrusting and enhanced subduction erosion (Kay et al., 1994, 2004, 2013; Goss et al., 2013). Adam and Reuther (2000) and Clift and Hartley (2007) also attributed uplift after 2 Ma to the onset of underplating and trenchward tectonic erosion. In Fig. 13a, the data point at 0.86 Ma reflects the highest emerged Pleistocene marine terrace in the Caldera Basin, at an elevation of 224 m (Quezada et al., 2007).

The overall uplift–subsidence–uplift pattern of the Bahía Inglesa Formation mirrors that of the Coquimbo Formation at Carizalillo and Tongoy (Figs. 1, 13b, 13c; Le Roux et al., 2005a, 2006), but these cycles were progressively more subdued towards the south. At Carrizalillo, subsidence after 15 Ma was followed by strong uplift commencing at around 12 Ma, whereas uplift started at 10.5 Ma in the Tongoy area. This was also attributed by Le Roux et al. (2005a) to the southward migration of a NE trending branch of the Juan Fernández Ridge (Yañez et al., 2001, 2002) past these localities. The Caldera Basin lies 140 km to the north of Carrizalillo, which suggests that the period between 15.3 and 10.4 Ma, when this part of the coastal sector was above sea level, might correspond to the presence of the ridge branch underneath the continental crust. This agrees with the presence of the JFR here at 12 Ma as postulated by Yañez et al. (2001).

Using the generalized curve (Fig. 13a), subsidence of the Caldera Basin in the wake of the migrating Juan Fernández Ridge started at about 11 Ma, whereas this process commenced at Carrizalillo at 7.5 Ma. Taking the 140 km distance between these two localities, this implies a southward migration rate for the Juan Fernández Ridge of around 4.0 cm/year. At Tongoy, subsidence commenced at 6.9 Ma and ended at 2.1 Ma (Le Roux et al., 2005b), which suggests a southward migration rate of about 26.5 cm/year between Carrizalillo and the former locality.

The amount of uplift attributed to the passing of the Juan Fernández Ridge was at least 100 m at Bahía Inglesa, 80 m at Carrizalillo, and 55 m at Tongoy, whereas the subsidence phase recorded around 350 m, 140 m, and 110 m at these three localities, respectively. This was subsequently followed by uplift, probably in part related to isostatic rebound, of about 250 m, 210 m, and 175 m in the same areas.

The slower migration rate in the north could possibly be related to the Serravalian–Tortonian cooling episode, attributed by Le Roux (2012) to a diminished South Pacific spreading rate accompanied by subsidence in central Chile (Le Roux et al., 2005a,b, 2006). However, this does not explain the increased intensity of uplift–subsidence–uplift cycles as compared to Carrizalillo and Tongoy.

It is likely that the elevation of the Juan Fernández Ridge branch was diminished by subduction erosion as it scraped against the bottom of the continental plate. Subduction erosion along the northern margin of the Chilean–Pampean flat-slab region is indicated by the presence of adakite-like high-Mg andesites containing a component of continental crust that was incorporated into the sub-arc mantle (Goss et al., 2013). However, a new portion of the ridge, as yet unaffected by subduction erosion, would be arriving at the trench as it progressively migrated south, so that this not only fails to explain the diminishing uplift–subsidence cycles, but also the dramatic increase in its migration rate. An alternative interpretation could be the effects of oroclinal bending of the Juan Fernández Ridge against the South American continental plate. If the ridge was originally oriented at a relatively high angle with the edge of the latter, its rate of southward migration would have been much slower (Le Roux et al., 2005a). At the same time, the stress field around the impact zone would be more concentrated (see northern bracket in Fig. 14), leading to more pronounced and rapid isostatic reactions. During the southward migration of the ridge, friction with the overlying continental plate could have led to its oroclinal bending, decreasing the angle of incidence and thus increasing the rate of southward migration. The stress field would also become broader but less intense (southern bracket in Fig. 14), with more subdued subsidence and isostatic rebound (Fig. 14).

A similar process of uplift–subsidence–uplift involving several hundreds of meters at Lima, Peru, was attributed by Le Roux et al. (2000) to the passage of the Nazca Ridge underneath the continental plate during the late Miocene. The present extension of this ridge also coincides with the absence of Quaternary volcanism in southern Peru (Isacks and Barazangi, 1977). Ridge subduction and migration therefore seems to be characterized by crustal updoming and thickening causing the cessation of volcanism, followed by crustal subsidence and stretching accompanied by renewed volcanism, and final uplift partly explained by mantle rebound. The angle of incidence between the subducting ridge and the edge of the continental plate can decrease due to oroclinal bending as a result of friction at the base of the latter, which would lead to an increased migration rate and less intense uplift–downward–uplift cycles.

## Acknowledgements

The authors are greatly indebted to financial and logistical support from Projects Fondecyt 1010691 and 130006, National Geographic Society Committee on Research Exploration grants 8903-11 and 9019-11, and Project CONICYT/FONDAP 15090013. Two anonymous reviewers are thanked for their critical but very constructive comments.

## Appendix A. Supplementary data

Supplementary data to this article can be found online at http://dx.doi.org/10.1016/j.sedgeo.2015.12.003.

## References

Achurra, L.E., 2004. Cambios del nivel del mar y evolución tectónica de la cuenca neógena de Caldera, III Región. Masters Thesis (unpubl.), Universidad de Chile, Santiago, 138 pp.

Achurra, L.E., Lacassie, J.P., Le Roux, J.P., Marquardt, C., Belmar, M., Ruiz-del-Solar, J., Ishman, S.E., 2009. Manganese nodules in the Miocene Bahía Inglesa Formation, north-central Chile: petrography, geochemistry, genesis and palaeoceanographic significance. Sedimentary Geology 217, 128–139.

Adam, J., Reuther, C.-D., 2000. Crustal dynamics and active fault mechanics during subduction erosion. Application of frictional wedge analysis on to the North Chilean Forearc. Tectonophysics 321, 297–325.

Álvarez, O., Gimenez, M., Folguera, A., Spagnotto, S., Bustos, E., Baez, W., Braitenberg, C., 2015. New evidence about the subduction of the Copiapó ridge beneath South America, and its connection with the Chilean–Pampean flat slab, tracked by satellite GOCE and EGM2008 models. Journal of Geodynamics 91, 65–88.

Bianucci, G., Sorbi, S., Suárez, M.E., Landini, W., 2006. The southernmost Sirenian record in the eastern Pacific Ocean, from the Late Miocene of Chile. Comptes Rendus Palevol 5, 945–952.

Bissig, T., Clark, A.H., Lee, J.K.W., Hodgson, C.J., 2002. Miocene landscape evolution and geomorphologic controls on epithermal processes in the El Indio-Pascua Au–Ag–Cu Belt, Chile and Argentina. Economic Geology 97, 971–996.

Blatt, H., Middleton, G., Murray, R., 1972. Origins of Sedimentary Rocks. Prentice Hall Inc, Englewood Cliffs, N.J, p. 634.

Bolli, H.M., Saunders, J.B., Perch-Nielsen, K., 1985. Plankton StratigraphyCambridge Earth Science Series vol. 1. University of Cambridge (214 pp.).

Buatois, L.A., Mángano, M.G., Aceñolaza, F.G., 2002. Trazas Fósiles: Señales de Comportamiento en el Registro Estratigráfico. Museo Paleontológico Egidio Feruglio, Chubut, Argentina, p. 381.

Buck, S., Goldring, R., 2003. Conical sedimentary structures, trace fossils or not? Observations, experiments, and review. Journal of Sedimentary Research 73, 338–353.

Camacho, H., Busby, C., Kneller, B., 2002. A new depositional model for the classical turbidite locality at San Clemente State Beach. California. American Association of Petroleum Geology Bulletin 86, 1543–1560.

Cande, S.C., Leslie, R.B., 1986. Late Cenozoic tectonics of the southern Chile trench. Journal of Geophysical Research 91, 471–496.

Carreño, C.A., 2012. Ambiente deposicional de la Formación Bahía Inglesa (Neógeno) en la Cuenca de Caldera, III Región, Chile. Graduate Thesis (unpubl.), Universidad de Chile, Santiago, 98 pp.

Chavez, M., 2008. Propiedades tafonómicas de la Ornitofauna del Miembro Bonebed de la Formación Bahía Inglesa, Atacama, Chile. Resumenes, III Congreso Latinoamericano de Paleontología de Vertebrados. Neuquén p. 55.

Clift, P.D., Hartley, A.J., 2007. Slow rates of subduction erosion and coastal underplating along the Andean margin of Chile and Peru. Geology 35, 503–506.

Culver, S.J., Buzas, M.A., 1980. Distribution of recent benthic foraminifera off the North American Atlantic Coast. Smithsonian Contributions to the Marine Sciences 6 (512 pp.).

Ehret, D.J., Macfadden, B.J., Jones, D.S., DeVries, T.J., Foster, D.A., Salas-Gismondi, R., 2012. Origin of the white shark *Carcharodon* (Lamniformes: Lamnidae) based on recalibration of the Upper Neogene Pisco Formation of Peru. Palaeontology 55, 1139–1153.

Elgueta, S., McDonough, M., Le Roux, J.P., Urqueta, E., Duhart, P., 2000. Estratigrafía y Sedimentología de las Cuencas Terciarias de la Región de los Lagos (39–41°30′S). Boletín No. 57. Servicio Nacional de Geología y Minería, Santiago (50 pp.).

Encinas, A., 2006. Estratigrafía y Sedimentología de los depósitos marinos mio-pleistocenos del área de navidad (33°00′- 34°30′S), Chile central: Implicaciones con respecto a la tectónica de antearco. Ph.D. thesis (unpubl.), Universidad de Chile, 177 pp.

Encinas, A., Finger, K., Nielsen, S., Lavenu, A., Buatois, L., Peterson, D., Le Roux, J.P., 2008. Rapid and major coastal subsidence during the Late Miocene in south-central Chile. Journal of South American Earth Sciences 25, 157–175.

Encinas, A., Fourtanier, E., Finger, K.L., Buatois, L.A., Le Roux, J.P., 2010. Stratigraphic implications of latest middle Miocene to earliest late Miocene diatoms in the Navidad Formation at Lo Abarca, central Chile (33°30′S). Ameghiniana 47, 527–533.

Encinas, A.. Finger, K.L., Nielsen, S.N., Contardo, X., Comment on Reply to Comment of Finger et al. (2013) on: 'Evidence for an Early-Middle Miocene age of the Navidad Formation (central Chile): Paleontological, paleoclimatic and tectonic implications'of Gutiérrez et al. (2013), Andean Geology 40 (1): 66-78). Andean Geology 41 (3), 2014, 635–656

Finger, K.L., Nielsen, S.N., DeVries, T.J., Encinas, A., Peterson, D.E., 2007. Paleontologic evidence for sedimentary displacement in Neogene forearc basins of central Chile. Palaios 22, 3–16.

Finger, K.L., Encinas, A., Nielsen, S.N., 2013. Comment on 'Evidence for an Early-Middle Miocene age of the Navidad Formation (central Chile): Paleontological, paleoclimatic and tectonic implications' of Gutiérrez et al. (2013, Andean Geology, 40 (1), 66–78). Andean Geology 40 (3), 571–579.

Gabalda, G., Nalpas, T., Bonvalot, S., 2005. The base of the Atacama Gravels Formation (26°S, northern Chile): first results from gravity data. Extended Abstracts, 6th International Symposium on Andean Geodynamics, Barcelona, pp. 286–289.

Galloway, J.J., Wissler, S.G., 1927. Pleistocene Foraminifera from the Lomita quarry, Palos Verdes Hills, California. Journal of Paleontology 1, 35–87.

Garrison, R., 1992. Neogene phosphogenesis along the eastern margin of the Pacific Ocean. Revista Geológica de Chile 19, 91–111.

Ghosh, P., Garzione, C.N., Eiler, J.M., 2006. Rapid uplift of the Altiplano revealed through $^{13}C\backslash^{18}O$ bonds in paleosol carbonates. Science 311, 511–515.

Godoy, E., Lara, L., 1998. Hojas Chañaral y Diego de Almagro, Región de Atacama. Servicio Nacional de Geología y Minería, Santiago.

Godoy, E., Marquardt, C., Blanco, N., 2003. Carta Caldera, Región de Atacama. Serie Geología Básica, No. 76. Servicio Nacional de Geología y Minería, Santiago (38 pp.).

Gómez, C.A., 2003. Cambios relativos del nivel del mar durante el Cenozoico tardío, en la zona de Carrizalillo, III Región, Chile. Masters thesis (unpubl.), Universidad de Chile, Santiago, 112 pp.

Goss, A.R., Kay, S.M., Mpodozis, C., 2013. Andean adakite-like high-Mg andesites on the northern margin of the Chilean–Pampean flat-slab (27–28.5°S) associated with frontal arc migration and fore-arc subduction erosion. Journal of Petrology 54, 2193–2234.

Gregory-Wodziki, K.M., 2000. Uplift history of the Central and Northern Andes: a review. Geological Society of America Bulletin 112, 1091–1105.

Gross, O., 2001. Foraminifera. In: Costello, M.J. (Ed.), European register of marine species: a check-list of the marine species in Europe and a bibliography of guides to their identification. Collection Patrimoines Naturels 50, pp. 60–75.

Gutiérrez, N.M., 2011. Diversidad y cambios florísticos durante el Mioceno en Chile central. Masters Thesis (Unpubl.), Universidad de Chile, 70 pp.

Gutiérrez, N.M., Hinojosa, L.F., Le Roux, J.P., Pedroza, V., 2013. Evidence for an Early–Middle Miocene age of the Navidad Formation (central Chile): paleontological, paleoclimatic and tectonic implications. Andean Geology 40, 66–78.

Gutstein, C., Rubilar-Rogers, D., Suárez, M.E., 2007. Nuevo yacimiento con vertebrados fósiles del Neógeno del desierto de Atacama (Formación Bahía Inglesa). Resumenes (on CD). GEOSUR, Santiago.

Gutstein, C.S., Yuri, R.Y., Soto, S., Suárez, M.E., Rubilar-Rogers, D.E., 2008. La fauna de vertebrados fósiles del "bonebed" de la Formación Bahía Inglesa y aspectos taxonómicos. Actas del I Simposio–Paleontología en Chile. MNHN, pp. 102–108.

Gutstein, C.S., Cozzuol, M.A., Vargas, A.O., Suárez, M.E., Schultz, C.L., Rubilar-Rogers, D., 2009. Patterns of skull variation of Brachydelphis (Cetacea, Odontoceti) from the Neogene of the Southeastern Pacific. Journal of Mammalogy 90, 504–519.

Gutstein, C.S., Horwitz, E., Valenzuela-Toro, A., Figueroa-Bravo, C.P., 2015. Cetáceos fósiles de Chile: contexto evolutivo y paleobiogeográfico. In: Rubilar-Rogers, D., Otero, R., Vargas, A.O., Sallaberry, M. (Eds.), Los Vertebrados fósiles de Chile. Publicación Ocasional Museo Nacional de Historia Natural N°63 (467 pp.).

Guzmán, N., Marquardt, C., Ortlieb, L., Frassinetti, D., 2000. La malacofauna neógena y cuaternaria del área de Caldera (27°–28°S): Especies y rangos bioestratigráficos. Congreso Geológico Chileno, Puerto Varas vol. 1, pp. 476–481.

Hardenbol, J., Thierry, J., Farley, M.B., Jacquin, T., Graciansky, P.-C., Vial, P.R., 1998. Mesozoic and Cenozoic sequence chronostratigraphic framework of European basins. In: Graciansky, P.-C., et al. (Eds.), Mesozoic and Cenozoic sequence stratigraphy of European basins. SEPM (Society for Sedimentary Geology) Special Publication 60 (chart 1).

Hartley, A., Howell, J., Mather, A.E., Chong, G., 2001. A possible Plio-Pleistocene tsunami deposit, Hornitos, northern Chile. Revista Geologica de Chile 28, 117–125.

Hayward, B., 2015. In: Hayward, B.W., Cedhagen, T., Kaminski, M., Gross, O. (Eds.), *Virgulinella pertusa*. World Foraminifera Database.

Hedberg, H.D., 1976. International Stratigraphic Guide: A Guide to Stratigraphic Classification. Terminology and Procedure, by the International Subcommission on Stratigraphic Classification of IUGS Commission of Stratigraphy. Wiley Interscience Publication, New York (200 pp.).

Henríquez, A.A., 2006. Variaciones locales del nivel del mar en las cuencas neógenas de Caldera, III Región y Arauco, VIII Región: Deducción de tasas de alzamiento y subsidencia tectónica. Masters Thesis (unpubl.), Universidad de Chile, Santiago, 170 pp.

Herm, D., 1969. Marines Pliozän and Pleistozän in Nord- und Mittel.Chile unter besonderer Berücksichtigung der Entwicklung der Mollusken-Faunen. Zitteliana, München.

Howard, J., Mayou, T., Heard, R., 1977. Biogenic sedimentary structures formed by rays. Journal of Sedimentary Petrology 47, 339–346.

Isacks, B.L., Barazangi, M., 1977. Geometry of Benioff zones: lateral segmentation and downbending of the subducted lithosphere. In: Talwani, M., Pitman, W.C. (Eds.), Island Arcs, Deep-sea Trenches and Back-arc Basins. American Geophysical Union, Maurice Ewing Series 1, pp. 99–114.

Kay, S.M., Abbruzzi, J.M., 1996. Magmatic evidence for Neogene lithospheric evolution of the central Andean 'flat-slab' between 308S and 328S. Tectonophysics 259, 15–28.

Kay, S.M., Mpodozis, C., Tittler, A., Cornejo, P., 1994. Tertiary magmatic evolution of the Maricunga mineral belt in Chile. International Geology Review 36, 1079–1112.

Kay, S.M., Godoy, S., Kurtz, A., 2004. Episodic arc migration, crustal thickening, subduction erosion, and magmatism in the south-central Andes. Geological Society of America Bulletin 117, 67–88.

Kay, S.M., Mpodozis, C., Gardeweg, M., 2013. Magma sources and tectonic setting of Central Andean andesites (25°58′–28°8′S) related to crustal thickening, fore-arc subduction erosion and delamination. In: Gomez-Tuena, A., et al. (Eds.), Orogenic Andesites and Crustal Growth. Geological Society, London, Special Publications 385.

Le Roux, J.P., 2012. A review of Tertiary climate changes in southern South America and the Antarctic Peninsula. Part 1: Oceanic conditions. Sedimentary Geology 247 (248), 1–20.

Le Roux, J.P., 2015. A critical examination of evidence used to re-interpret the Hornitos mega-breccia as a mass-flow deposit caused by cliff failure. Andean Geology 42, 139–145.

Le Roux, J.P., Elgueta, S., 2000. Sedimentologic development of a Late Oligocene-Miocene forearc embayment, Valdivia Basin Complex, southern Chile. Sedimentary Geology 130, 27–44.

Le Roux, J.P., Tacares Correa, C., Alayza, F., 2000. Sedimentology of the Rímac-Chillón alluvial fan at Lima, Peru, as related to Plio-Pleistocene sea-level changes, glacial cycles and tectonics. Journal of South American Earth Sciences 13, 499–510.

Le Roux, J.P., Gómez, C., Fenner, J., Middleton, H., 2004. Sedimentological processes in a scarp-controlled rocky shoreline to upper continental slope environment, as revealed by unusual sedimentary features in the Neogene Coquimbo Formation, north-central Chile. Sedimentary Geology 165, 67–92.

Le Roux, J.P., Gómez, C.A., Olivares, D.M., Middleton, H., 2005a. Determining the Neogene behavior of the Nazca Plate by geohistory analysis. Geology 33, 165–168.

Le Roux, J.P., Gómez, C., Venegas, C., Fenner, J., Middleton, H., Marchant, M., Buchbinder, B., Frassinetti, D., Marquardt, C., Gregory-Wodzicki, K.M., Lavenu, A., 2005b. Neogene-Quaternary coastal and offshore sedimentation in north-central Chile: record of sea level changes and implications for Andean tectonism. Journal of South American Earth Sciences 19, 83–98.

Le Roux, J.P., Olivares, D.M., Nielsen, S.N., Smith, N.D., Middleton, H., Fenner, J., Ishman, S.E., 2006. Bay sedimentation as controlled by regional crustal behaviour, local tectonics and eustatic sea-level changes: Coquimbo Formation (Miocene-Pliocene), Bay of Tongoy, central Chile. Sedimentary Geology 184, 133–153.

Le Roux, J.P., Nielsen, S.N., Kemnitz, H., Henriquez, A., 2008. A Pliocene mega-tsunami deposit and associated features in the Ranquil Formation, southern Chile. Sedimentary Geology 203, 164–180.

Le Roux, J.P., Gutiérrez, N.M., Hinojosa, L.F., Pedroza, V., Becerra, J., 2013. Reply to "Comment on: Evidence for an Early–Middle Miocene age of the Navidad Formation (central Chile): paleontological, paleoclimatic and tectonic implications (Andean Geology, 49, 66-78)". Andean Geology 40, 580–588.

Le Roux, J.P., Gutiérrez, N.M., Hinojosa, F., Becerra, J., Pedroza, V., 2014. Reply to Comment of Encinas et al. (2014) on: 'Evidence for an Early–Middle Miocene age of the Navidad Formation (central Chile): Paleontological, climatic and tectonic implications' of Gutiérrez et al. (2013, Andean Geology, 40 (1), 66-78). Andean Geology 41, 657–669.

Long, D.J., 1993. Late Miocene and Early Pliocene fish assemblages from the north central coast of Chile. Tertiary Research 14, 117–126.

Marchant, M., Marquardt, C., Blanco, N., Godoy, E., 2000. Foraminíferos del área de Caldera (26°45′–28°S) y su utilización como indicadores cronoestratigráficos del Neógeno. IX Congreso Geológico Chileno vol. 1, pp. 499–503.

Marquardt, C., 1999. Neotectónica de la franja costera y aportes a la geología regional entre Caldera y Caleta Pajonal (27°–27°45´), III Región de Atacama. Masters thesis (unpubl.), Universidad de Chile, Santiago.

Marquardt, C., Blanco, N., Godoy, E., Lavenu, A., Ortlieb, L., Marchant, M., Guzmán, N., 2000. Estratigrafía del Cenozoico superior en el área de Caldera (26°45′28″S), III Región de Atacama, Chile. IX Congreso Geológico Chileno, Puerto Varas vol. 2, pp. 504–508.

Marquardt, C., Lavenu, A., Artlieb, L., Godoy, E., Comte, D., 2004. Coastal neotectonics in Southern Central Andes: uplift and deformation of marine terraces in northern Chile (27°S). Tectonophysics 394, 193–219.

Mortimer, C., 1969. The geomorphological evolution of the southern Atacama Desert, Chile. Ph.D. thesis (unpubl.), University College, London.

Mortimer, C., 1973. The Cenozoic history of the southem Atacama Desert, Chile. Journal of the Geological Society of London 129, 505–526.
Mpodozis, C., Cornejo, P., Kay, S.M., Tittler, A., 1995. La Franja de Maricunga: Síntesis de la evolución del frente volcánico Oligoceno-Mioceno de la zona sur de los Andes Centrales. Revista Geologica de Chile 22, 273–314.
Nigam, R., Anantha Padmanabha Setty, M.G., 1982. Ecological regimen and distribution of *Virgulinella* spp. in the inshore sediments of Western India. Palaeogeography, Palaeoclimatology, Palaeoecology 38, 57–61.
Nomura, R., 1982. List and bibliography of the recent benthonic foraminifera of Japan, 1925–1981. Memoirs of the Faculty of Education, Shimane University 16, 21–54.
Nur, A., Avraham, B., 1981. Volcanic gaps and the consumption of aseismic ridges in South America. Memoir - Geological Society of America 154.
Pardo, M., Comte, D., Monfret, T., 2002. Seismotectonic and stress distribution in the central Chile subduction zone. Journal of South American Earth Sciences 15, 11–22.
Polovodova Asteman, I., Nordberg, K., 2013. Foraminiferal fauna from a deep basin in Gullmar Fjord: the influence of seasonal hypoxia and North Atlantic Oscillation. Journal of Sea Research 79, 40–49.
Pyenson, N.D., Gutstein, G.S., Parham, J.F., Le Roux, J.P., Carreño, C., Little, H., Metallo, A., Rossi, V., Valenzuela-Toro, A.M., Velez-Juarbe, J., Santelli, C.M., Rubilar Rogers, D., Cozzuol, M.A., Suarez, M.E., 2014. Repeated mass strandings of Miocene marine mammals from Atacama Region of Chile point to sudden death at sea. Proceedings of the Royal Society B: Biological Sciences 281, 20133316.
Quezada, J., González, G., Dunai, T., Jensen, A., Juez-Larré, J., 2007. Pleistocene littoral uplift of northern Chile: $^{21}$Ne age of the upper marine terrace of Caldera-Bahía Inglesa area. Revista Geologica de Chile 34, 81–96.
Rea, D.K., 1976. Analysis of a fast-spreading rise-crest: the East Pacific Rise, 9°–12° south. Marine Geophysical Researches 2, 291–313.
Rojo, M., 1985. Un aporte al conocimiento del terciario marino: Formación Bahía Inglesa. IV Congreso Geológico Chileno, Universidad del Norte, Antofagasta vol. 1, pp. 514–531.
Rubilar-Rogers, D., Gutstein, C., Mourgues, F., 2009. Nuevo yacimiento con vertebrados fósiles de la Formación Bahía Inglesa (Mioceo-Plioceno) del norte de Chile. Fondo de Apoya a la Investigación Patrimonial (Unpubl. Report), p. 7-23.
Sallaberry, M., Rubilar-Rogers, D., Suárez, M.E., Gutstein, C., 2007. The skull of a fossil prion (Aves: Procellariiformes) from the Neogene (Late Miocene) of northern Chile. Revista Geologica de Chile 34, 147–154.
Siesser, W.G., Rogers, J., 1976. Authigenic pyrite and gypsum in South West African continental slope sediments. Sedimentology 23, 567–577.
Spiske, M., Bahlburg, H., Weiss, R., 2014. Pliocene mass failure deposits mistaken as submarine tsunami backwash sediments—an example from Hornitos, northern Chile. Sedimentary Geology 305, 69–82.
Srinivasan, M., Kennett, J., 1981. Neogene planktonic foraminiferal biostratigraphy and evolution: Equatorial to subantarctic, South Pacific. Marine Paleontology 6 (1981), 499–533.
Suárez, M.E., 2015. Tiburones, rayas y quimeras fósiles de Chile. In: Rubilar-Rogers, D., Otero, R., Vargas, A.O., Sallaberry, M. (Eds.), Los vertebrados fósiles de Chile. Publicación Ocasional del Museo Nacional de Historia Natural, Santiago, Chile 63, pp. 17–33.
Suárez, M.E., Chávez, M., Marquardt, C., 2002. Nuevos hallazgos de vertebrados marinos la Formación Bahía Inglesa (Mioceno-Plioceno) Caldera, norte de Chile. Actas, I Congreso Latinoamericano de Paleontología de Vertebrados, Santiago, Chile, pp. 50–51.
Suárez, M.E., Lamilla, J., Marquardt, C., 2004. Peces Chimaeriformes (Chondrichthyes, Holocephali) del Neógeno de la Formación Bahía Inglesa (Región de Atacama, Chile). Revista Geologica de Chile 31, 105–117.
Suárez, M.E., Encinas, A., Ward, D., 2006. An Early Miocene elasmobranch fauna from the Navidad Formation, Central Chile, South America. Cainozoic Research 4, 3–18.
Suárez, M.E., Valenzuela-Toro, A., Yury-Yáñez, R., 2010. Primer yacimiento con vertebrados marinos del Pleistoceno en Caldera, Región de Atacama, Chile. Actas, II Simposio Paleontología en Chile, Concepción, Chile, pp. 64–65.
Valenzuela-Toro, A., Gutstein, C.S., 2015. Mamíferos marinos fósiles (excepto Cetacea) de Chile. In: Rubilar-Rogers, D., Otero, R., Vargas, A.O., Sallaberry, M. (Eds.), Los Vertebrados fósiles de Chile. Publicación Ocasional Museo Nacional de Historia Natural N°63 (467 pp.).
Valenzuela-Toro, A., Gutstein, C.S., Varas-Malca, R.M., Suárez, M.E., Pyenson, N.D., 2013. Pinniped turnover in the South Pacific Ocean: new evidence from the Plio-Pleistocene of the Atacama Desert, Chile. Journal of Vertebrate Paleontology 33, 216–223.
Van Hinte, J.E., 1978. Geohistory analysis: application of micropaleontology in exploration geology. American Association of Petroleum Geologists Bulletin 62, 201–222.
Walsh, S.A., Hume, J., 2001. A new Neogene marine avian assemblage from north-central Chile. Journal of Vertebrate Paleontology 21, 484–491.
Walsh, S.A., Martill, D.M., 2006. A possible earthquake-triggered mega-boulder slide in a Chilean Mio-Pliocene marine sequence: evidence for rapid uplift and bonebed genesis. Journal of the Geological Society of London 163, 697–705.
Walsh, S., Naish, D., 2002. Fossil seals from late Neogene deposits in South America: a new pinniped (carnivora, mammalia) assemblage from Chile. Paleontology 45, 821–842.
Walsh, S.A., Suárez, M., 2005. First post-Mesozoic record of Crocodyliformes from Chile. Acta Palaeontologica Polonica 50 (3), 595–600.
Walsh, S.A., Suárez, M.E., 2006. New penguin remains from the Pliocene of northern Chile. Historical Biology 18, 115–126.
Yañez, G., Ranero, C.R., Von Huene, R., Díaz, J., 2001. Magnetic anomaly interpretation across the southern central Andes (32ø-34øSß). The role of the Juan Fernandez Ridge in the late Tertiary evolution of the margin. Journal of Geophysical Research 106, 6325–6345.
Yañez, G., Cembrano, J., Pardo, M., Ranero, C., Selles, D., 2002. The Challenger–Juan Fernández–Maipo major tectonic transition of the Nazca–Andean subduction system at 33–348: geodynamic evidence and implications. Journal of South American Earth Sciences 15, 23–38.